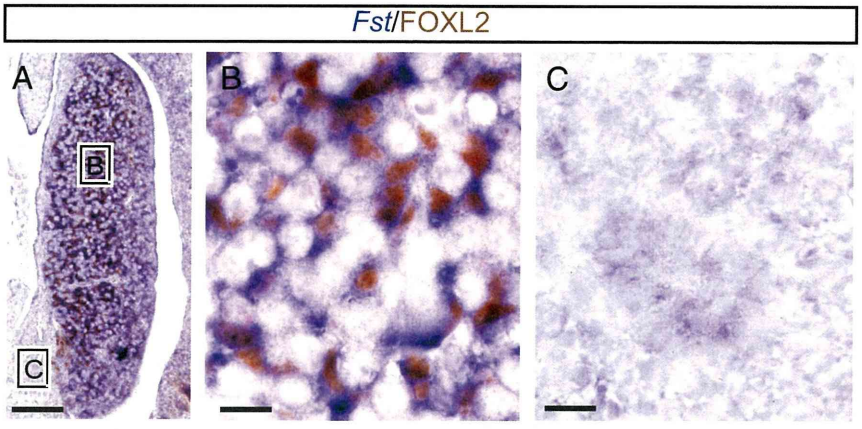

FIG. 2. *Fst* and FOXL2 colocalize in fetal ovaries. *In situ* hybridization (*Fst, purple*) and immunohistochemistry (FOXL2, *brown*) on sagittal section of 13.5 dpc ovary. A, Low-power image of whole ovary. B, High-power image of ovary showing coexpression of *Fst* mRNA and FOXL2 protein in the same cells. C, Adjacent negative control tissue (mesonephros) expressing neither *Fst* nor FOXL2. The *rectangular areas* in panel A indicate the location of panels B and C. *Scale bars*, 200 μm (A); 40 μm (B and C).

Using the same *in vitro* model system, *Foxl2* expression was unaffected by BMP2 (Fig. 3E), whereas *Bmp2* was up-regulated by FOXL2 (Fig. 3F). These data suggest that FOXL2 may exert its effects on *Fst* expression in the ovary through a combination of direct activation of the *Fst* promoter, cooperative interaction with one or more SMADs, and enhanced transcription of the gene encoding BMP2. To elucidate whether the regulation of *Bmp2* by FOXL2 is essential for *Fst* up-regulation, we used BMP2 antagonist Noggin in KK1 cell culture. Noggin is a TGF-β binding protein that antagonizes TGF-β molecule function by interrupting its binding to receptors and plays an important role in dorsoventral patterning, limb formation, and neural tube morphogenesis during embryonic development (37). In KK1 cells, Noggin abrogated the *Fst* regulation by BMP2 in a dose-dependent manner (Fig. 4A), as expected. In the presence of Noggin, FOXL2 retained the ability to up-regulate *Fst* expression in KK1 cells (Fig. 4B), indicating that the up-regulation of *Fst* by FOXL2 likely occurs through a combination of direct effects on *Fst* expression and indirect effects mediated by up-regulation of *Bmp2*.

BMP2 up-regulates *Fst* expression *ex vivo*

Based on the *in vitro* data, we analyzed cultures of organ explants to elucidate the regulation of *Fst in vivo*. Mouse embryonic gonads were dissected at 11.5 dpc and cultured in medium containing BMP2 in the presence or absence of the inhibitor Noggin. Gene expression changes were evaluated by qRT-PCR. Incubation of XX genital ridges for 48 h with 500 ng/ml BMP2 resulted in strong up-regulation of *Fst* expression (Fig. 5A). Lower concentration of BMP2 (100 ng/ml) and shorter incubation time (3, 6, and 24 h) did not significantly up-regulate *Fst* expression (data not shown). In contrast, BMP2 did not up-regulate *Foxl2* in cultured fetal ovaries (Fig. 5B). In agreement with our findings using KK1 cells, Noggin abrogated the action of BMP2 in stimulating *Fst* expression (Fig. 5A). Furthermore, *Fst* expression was up-regulated by exogenous BMP2 only in XX gonads, not in XY gonads (Fig. 5A), presumably because the latter lack endogenous *Foxl2* expression.

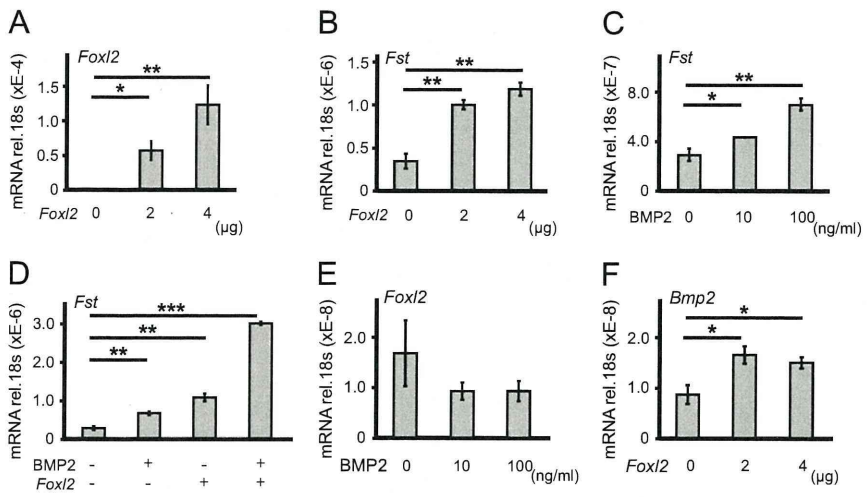

FIG. 3. FOXL2 and BMP2 cooperatively up-regulate *Fst* expression in KK1 cells. qRT-PCR analysis of *Foxl2*, *Fst*, *Bmp2* mRNA levels in KK1 granulosa-like cells transfected with constructs expressing with *Foxl2* (A, B, and F: 0, 2, and 4 μg), treated with BMP2 (C and E: 0, 10, 100 ng/ml), or treated with BMP2 (D: 100 ng/ml) and/or *Foxl2* expression plasmid (D: 4 μg). Data sets represent mRNA expression relative to 18S (mean ± SEM of three biologically independent experiments performed in triplicate). *Asterisks* indicate level of statistical significance (*, $P < 0.05$; **, $P < 0.01$; ***, $P < 0.001$).

In vivo requirements for *Fst* up-regulation

For further investigation of *Fst* gene regulation *in vivo*, we analyzed *Fst* gene expression in XX gonads of *Foxl2*-null knockout mice at different stages of development. *Fst* expression was significantly reduced in *Foxl2*-null mice at 13.5 dpc and P0 (Fig. 6A) and also at 16.5 dpc, confirming that FOXL2 is upstream of *Fst* expression during ovarian development *in vivo*.

Because loss of *Bmp2* function in mice is lethal during embryogenesis before sex is determined (4), we were unable to

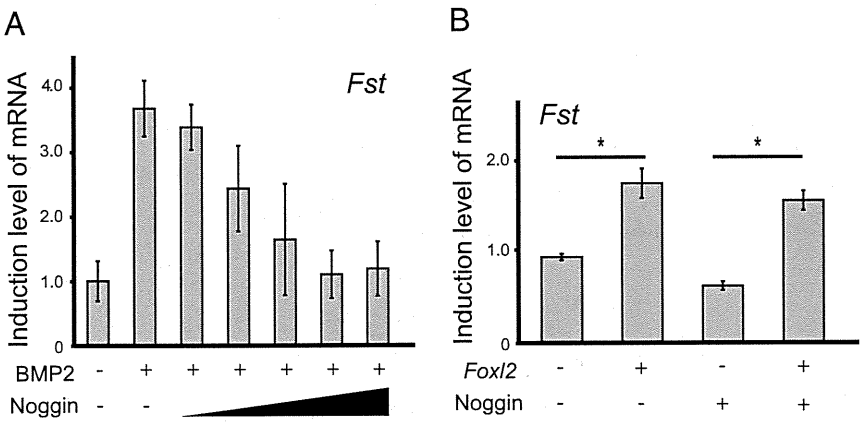

FIG. 4. FOXL2 is also able to up-regulate *Fst* independently of BMP2. A, BMP antagonist Noggin suppresses the BMP2-induced up-regulation of *Fst* expression in KK1 cells; *triangle* represents increasing concentrations of recombinant Noggin from 100 to 500 ng/ml. B, *Fst* expression in KK1 cells transfected with constructs expressing *Foxl2* (4 μg) and/or treated with Noggin (100 ng/ml). Data sets represent mRNA expression relative to 18S (mean ± SEM of three biologically independent experiments performed in triplicate). *Asterisks* indicate level of statistical significance (*, $P < 0.05$).

analyze the effect of *Bmp2* knockout on *Fst* expression. However, because WNT4 has previously been implicated in affecting *Fst* expression at 14.5 dpc (4, 12), we analyzed *Fst* gene expression in XX gonads of *Wnt4*-null, and *Foxl2*/*Wnt4* double knockout embryos at different stages of development. In *Wnt4*-null mice, *Fst* expression was remarkably reduced at 13.5 dpc, as reported previously (Fig. 6A) (4). However, *Fst* expression had fully recovered to wild-type levels by P0 (Fig. 6A). Analysis at the intervening time point of 15.5 dpc showed that most of the recovery had been achieved by this time (Fig. 6B). These data suggest that although WNT4 has an important role for *Fst* expression *in vivo*, its role is limited to the early phase of *Fst* expression during ovarian development.

Finally, *Foxl2*/*Wnt4* double knockout showed a complete loss of *Fst* expression comparable to that seen in wild-type XY gonads, at both 13.5 dpc and P0 (Fig. 6A), suggesting that a combination of WNT4 priming and BMP2/FOXL2 maintenance is required for *Fst* expression in the developing ovary.

Bmp2 requires *Foxl2* at P0

Our experiments involving KK1 cells indicated that FOXL2 is able to influence *Fst* gene expression through a combination of direct effects on *Fst* and indirect effects mediated by up-regulation of *Bmp2*. To examine the possible regulation of *Bmp2* by FOXL2 *in vivo*, we analyzed *Bmp2* gene expression in XX gonads of *Foxl2*-null mice at a range of stages. *Bmp2* expression was significantly reduced in *Foxl2*-null mice at P0 (Fig. 6C), but not at 13.5 or 16.5 dpc (Fig. 6, C and D). This observation confirms that FOXL2 is upstream of *Bmp2* expression during ovarian development; however, its contribution is limited to later stages.

In contrast, in *Wnt4*-null mice, *Bmp2* expression was compromised at all three stages examined (13.5 dpc, 15.5 dpc, P0; Fig. 6D), consistent with published data (4). *Foxl2*/*Wnt4* double knockout showed significantly reduced *Bmp2* expression at both 13.5 dpc and P0, as expected (Fig. 6C).

Discussion

In previous reports, FOXL2 and WNT4 have been suggested to regulate *Fst* expression during ovarian development (4, 19, 20, 35, 38, 39). Our data suggest that BMP2 is another factor that regulates *Fst* expression and that it acts cooperatively with FOXL2. This is the first report to identify a molecular function for BMP2 during ovarian development.

Observations of genetically modified mice have hinted at a causal relationship between FOXL2 and *Fst* expression (17, 19, 35). Our present data extend these observations 1) by showing that *Fst* is coexpressed with FOXL2 in somatic cells during ovarian development, 2) by demonstrating that transfection of a granulosa-like cell line with FOXL2 expression construct augments *Fst* gene expression, and 3) by demonstrating that *Fst* expression is compromised in *Foxl2*-deficient mouse fetal ovaries. Our data thus strongly support

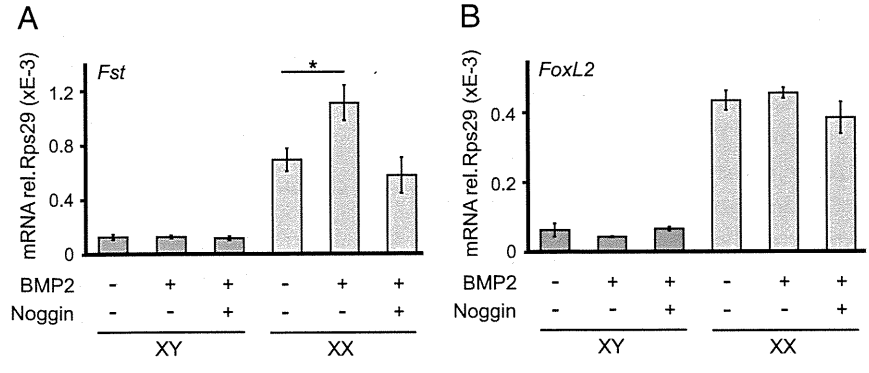

FIG. 5. BMP2 up-regulates *Fst* expression in *ex vivo* organ culture. *Fst* (A) and *Foxl2* (B) expression in *ex vivo* gonadal organ culture was evaluated by using qRT-PCR. Gonads (11.5 dpc) were cultured on the medium containing BMP2 (500 ng/ml), or BMP2 (500 ng/ml) and Noggin (2 μg/ml). Data represent mRNA expression relative to *Rps29* (mean ± SEM of three biologically independent experiments performed in triplicate). *, $P < 0.05$.

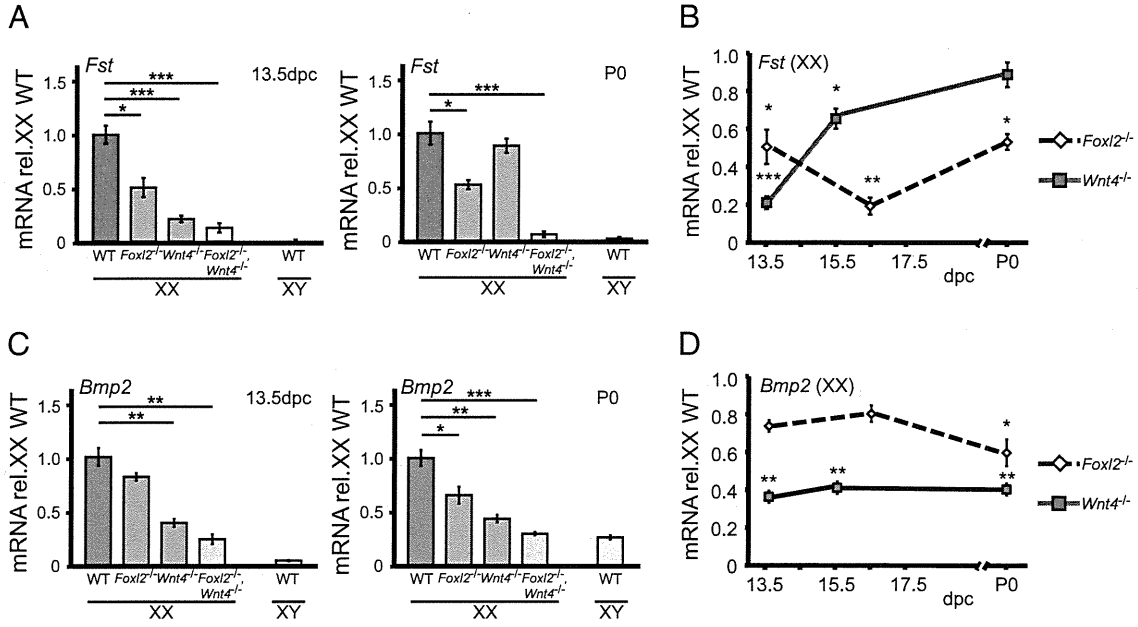

FIG. 6. *Fst* and *Bmp2* expression in *Foxl2*$^{-/-}$, *Wnt4*$^{-/-}$, and *Foxl2*$^{-/-}$/*Wnt4*$^{-/-}$ knockout mice. A, qRT-PCR analysis of *Fst* expression at 13.5 dpc and P0 in *Foxl2*$^{-/-}$, *Wnt4*$^{-/-}$, and *Foxl2*$^{-/-}$/*Wnt4*$^{-/-}$ XX gonads. B, Time course of *Fst* expression in *Foxl2*$^{-/-}$ and *Wnt4*$^{-/-}$ XX gonads. C, qRT-PCR analysis of *Bmp2* expression at 13.5 dpc and P0 in *Foxl2*$^{-/-}$, *Wnt4*$^{-/-}$, and *Foxl2*$^{-/-}$/*Wnt4*$^{-/-}$ XX gonads. D, Time course of *Bmp2* expression in *Foxl2*$^{-/-}$ and *Wnt4*$^{-/-}$ XX gonads. All time points analyzed are shown. Data represent mRNA expression relative to XX wild-type (WT) gonads (mean ± SEM of three biologically independent experiments performed in triplicate). *, $P < 0.05$; **, $P < 0.01$; ***, $P < 0.001$.

the conclusion that FOXL2 regulates *Fst* expression during fetal ovarian development.

In addition, the different temporal profiles of *Fst* and *Foxl2* expression that we observed implicate additional factor(s) in the regulation of *Fst* in ovaries. The observation that *Bmp2* and *Fst* have a very similar profile of expression during fetal ovary development suggests a major role for BMP2, and our finding that BMP2 up-regulates *Fst* expression in KK1 cells and in *ex vivo* organ culture of mouse fetal ovaries supports this conclusion. Several reports have shown a direct interaction between forkhead proteins and SMADs (24–27). Recently, it has been reported that FOXL2 and SMAD3 interact and synergistically up-regulate *Fst* expression in pituitary cells (21). Our *in vitro* data indicate that BMP2 and FOXL2 cooperatively stimulate *Fst* expression by *Foxl2* in fetal ovaries. This cooperative mechanism was also supported by the *ex vivo* organ culture analysis showing that BMP2 activated *Fst* expression in XX gonads, and not in XY gonads. The result suggests that a female-specific cofactor assisted BMP2 function, consistent with a role for endogenous FOXL2 as the cofactor. Overall, our data shed new light on the regulation of *Fst* expression and suggest that FOX/SMAD cooperativity may be a more general phenomenon in developmental biology.

We have added further complexity to this picture by using *Foxl2*-null mice and cultured cells to show that *Bmp2* expression is responsive to levels of FOXL2. Therefore, the observed effects of FOXL2 on *Fst* expression in the ovary may be mediated by a combination of direct activation of *Fst* transcription, interaction with one or more SMADs, and enhanced transcription of the gene encoding BMP2 (Fig. 7), although the contribution of the *Foxl2*-BMP2 pathway is likely to be limited, given the modestly reduced expression of *Bmp2* in *Foxl2*-knockout mice at P0 but not at 13.5 or 16.5 dpc. Considering the *Fst* and *Bmp2* expression levels at each stage in *Foxl2*-null mice, the contribution of each pathway changes in a stage-dependent manner. Further studies will be required to

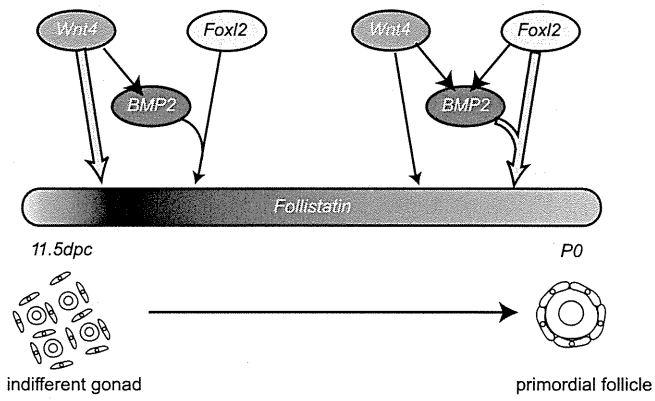

FIG. 7. Model for the regulation of *Fst* expression during ovarian development. At early stages such as 11.5 dpc, WNT4 likely acts as a major regulator for *Fst* expression. WNT4 also acts upstream of *Bmp2* and is required for the early phase of *Fst* expression (this study). Later in ovarian development (15.5 dpc to P0), FOXL2 and BMP2 are together required for *Fst* expression. BMP2 and FOXL2 up-regulate *Fst* expression cooperatively and individually, and FOXL2 also up-regulates *Bmp2* expression (this study).

identify the precise contribution of each pathway at each stage.

Our analyses also shed new light on the involvement of WNT4 in this system. At 13.5 dpc, *Fst* expression was markedly reduced in *Wnt4*-null mice but recovered thereafter. These observations suggest a new model in which WNT4 is likely to be important for the early stage (initiation) of *Fst* expression rather than for continued expression at later stages (maintenance). This model, depicted in Fig. 7, is strongly supported by the different expression profiles of *Wnt4* and *Fst* during ovarian development.

Considering the moderate impairment of the *Fst* expression in *Wnt4* and *Foxl2*-null mice, the decrease in *Fst* expression in double-knockout mice was more dramatic than expected. This phenomenon could be explained by the fact that XX gonads in double-knockout mice showed similarities to testes, with tubules and abundant expression of SOX9 and anti-Müllerian hormone (35) that were not observed in *Foxl2* or *Wnt4* single-knockout mice (16, 17, 35). Male-specific regulators such as SOX9 are known to suppress the ovarian developmental pathway (33), and it is therefore likely that *Sox9* up-regulation in the double mutant has an indirect effect on the expression of *Fst* in the double-knockout mice.

Our analysis of *Fst* expression in *Foxl2*- and *Wnt4*-knockout mice may also indicate a stage-dependent role for *Fst* in ovarian development. Previous studies have shown celomic vessel formation and germ cells survival are impaired in *Fst*-knockout embryos (4). *Wnt4*-null mice show a similar phenotype (12), and our present analysis shows that ablation of WNT4 function corresponds with loss of *Fst* expression at early stages (11.5 dpc) but not later stages (15.5 dpc and later). Conversely, in *Foxl2*-null gonads, which do not show ectopic celomic vessel formation or germ cell defects (17), *Fst* expression was higher at 11.5 dpc than at 15.5 dpc. These observations may indicate that the early expression of *Fst* is essential for inhibiting celomic vessel formation and ensuring survival of germ cells in XX gonads, although stage-specific ablation of *Fst* will be required to test this possibility.

In summary, our data suggest that FOXL2 and BMP2 regulate *Fst* expression cooperatively during fetal ovarian development. The contribution of WNT4, FOXL2, and BMP2 to the regulation of *Fst* is likely to be sequential and stage dependent. To initiate *Fst* expression, WNT4 appears to be the major regulator, whereas FOXL2 and BMP2 assume a more prominent role in maintenance of *Fst* expression. Our data contribute to a growing picture of the regulatory networks underpinning development of the mammalian ovary.

Acknowledgments

We thank I. Huhtaniemi (Imperial College London, UK) for providing KK1 cells. K.K., D.W., D.S., and P.K. conceived and designed the experiments. K.K., E.P., and H.C. performed the experiments and analyzed the data. K.K. and P.K. wrote the paper.

Address all correspondence and requests for reprints to: Peter Koopman, Institute for Molecular Bioscience, The University of Queensland, Brisbane, Queensland 4072, Australia. E-mail: p.koopman@uq.edu.au.

This work was supported by research grants from the Australian Research Council and National Health and Medical Research Council of Australia. D.W. is a Career Development Award II Fellow of the National Health and Medical Research Council. P.K. is a Federation Fellow of the Australian Research Council. This research was supported in part by the Intramural Research Program of the National Institutes of Health, National Institute on Aging.

Disclosure Summary: Neither the entire paper nor any part of its content has been published or has been accepted by another journal. The paper is not being submitted in its entirety or in part to any other journal. No sponsors were involved. There is no potential conflict of interest.

References

1. **Wilhelm D, Palmer S, Koopman P** 2007 Sex determination and gonadal development in mammals. Physiol Rev 87:1–28
2. **Koopman P, Gubbay J, Vivian N, Goodfellow P, Lovell-Badge R** 1991 Male development of chromosomally female mice transgenic for Sry. Nature 351:117–121
3. **Menke DB, Page DC** 2002 Sexually dimorphic gene expression in the developing mouse gonad. Gene Expr Patterns 2:359–367
4. **Yao HH, Matzuk MM, Jorgez CJ, Menke DB, Page DC, Swain A, Capel B** 2004 Follistatin operates downstream of Wnt4 in mammalian ovary organogenesis. Dev Dyn 230:210–215
5. **Phillips DJ, de Kretser DM** 1998 Follistatin: a multifunctional regulatory protein. Front Neuroendocrinol 9:287–322
6. **Shimasaki S, Koga M, Buscaglia ML, Simmons DM, Bicsak TA, Ling N** 1989 Follistatin gene expression in the ovary and extragonadal tissues. Mol Endocrinol 3:651–659
7. **Matzuk MM, Lu N, Vogel H, Sellheyer K, Roop DR, Bradley A** 1995 Multiple defects and perinatal death in mice deficient in follistatin. Nature 374:360–363
8. **Robertson DM, Klein R, de Vos FL, McLachlan RI, Wettenhall RE, Hearn MT, Burger HG, de Kretser DM** 1987 The isolation of polypeptides with FSH suppressing activity from bovine follicular fluid which are structurally different to inhibin. Biochem Biophys Res Commun 149:744–749
9. **Ueno N, Ling N, Ying SY, Esch F, Shimasaki S, Guillemin R** 1987 Isolation and partial characterization of follistatin: a single-chain Mr 35,000 monomeric protein that inhibits the release of follicle-stimulating hormone. Proc Natl Acad Sci USA 84:8282–8286
10. **Jorgez CJ, Klysik M, Jamin SP, Behringer RR, Matzuk MM** 2004 Granulosa cell-specific inactivation of follistatin causes female fertility defects. Mol Endocrinol 18:953–967
11. **Muttukrishna S, Tannetta D, Groome N, Sargent I** 2004 Activin and follistatin in female reproduction. Mol Cell Endocrinol 225: 45–56
12. **Vainio S, Heikkilä M, Kispert A, Chin N, McMahon AP** 1999 Fe-

male development in mammals is regulated by Wnt-4 signalling. Nature 397:405–409
13. **Mandel H, Shemer R, Borochowitz ZU, Okopnik M, Knopf C, Indelman M, Drugan A, Tiosano D, Gershoni-Baruch R, Choder M, Sprecher E** 2008 SERKAL syndrome: an autosomal-recessive disorder caused by a loss-of-function mutation in WNT4. Am J Hum Genet 82:39–47
14. **Crisponi L, Deiana M, Loi A, Chiappe F, Uda M, Amati P, Bisceglia L, Zelante L, Nagaraja R, Porcu S, Ristaldi MS, Marzella R, Rocchi M, Nicolino M, Lienhardt-Roussie A, Nivelon A, Verloes A, Schlessinger D, Gasparini P, Bonneau D, Cao A, Pilia G** 2001 The putative forkhead transcription factor FOXL2 is mutated in blepharophimosis/ptosis/epicanthus inversus syndrome. Nat Genet 27:159–166
15. **Pailhoux E, Vigier B, Chaffaux S, Servel N, Taourit S, Furet JP, Fellous M, Grosclaude F, Cribiu EP, Cotinot C, Vaiman D** 2001 A 11.7-kb deletion triggers intersexuality and polledness in goats. Nat Genet 29:453–458
16. **Uda M, Ottolenghi C, Crisponi L, Garcia JE, Deiana M, Kimber W, Forabosco A, Cao A, Schlessinger D, Pilia G** 2004 Foxl2 disruption causes mouse ovarian failure by pervasive blockage of follicle development. Hum Mol Genet 13:1171–1181
17. **Schmidt D, Ovitt CE, Anlag K, Fehsenfeld S, Gredsted L, Treier AC, Treier M** 2004 The murine winged-helix transcription factor Foxl2 is required for granulosa cell differentiation and ovary maintenance. Development 131:933–942
18. **Kocer A, Pinheiro I, Pannetier M, Renault L, Parma P, Radi O, Kim KA, Camerino G, Pailhoux E** 2008 R-spondin1 and FOXL2 act into two distinct cellular types during goat ovarian differentiation. BMC Dev Biol 8:36
19. **Garcia-Ortiz JE, Pelosi E, Omari S, Nedorezov T, Piao Y, Karmazin J, Uda M, Cao A, Cole SW, Forabosco A, Schlessinger D, Ottolenghi C** 2009 Foxl2 functions in sex determination and histogenesis throughout mouse ovary development. BMC Dev Biol 9:36
20. **Ottolenghi C, Omari S, Garcia-Ortiz JE, Uda M, Crisponi L, Forabosco A, Pilia G, Schlessinger D** 2005 Foxl2 is required for commitment to ovary differentiation. Hum Mol Genet 14:2053–2062
21. **Blount AL, Schmidt K, Justice NJ, Vale WW, Fischer WH, Bilezikjian LM** 2009 FoxL2 and Smad3 coordinately regulate follistatin gene transcription. J Biol Chem 284:7631–7645
22. **Zhang H, Bradley A** 1996 Mice deficient for BMP2 are nonviable and have defects in amnion/chorion and cardiac development. Development 122:2977–2986
23. **Pangas SA, Li X, Umans L, Zwijsen A, Huylebroeck D, Gutierrez C, Wang D, Martin JF, Jamin SP, Behringer RR, Robertson EJ, Matzuk MM** 2008 Conditional deletion of Smad1 and Smad5 in somatic cells of male and female gonads leads to metastatic tumor development in mice. Mol Cell Biol 28:248–257
24. **Chen X, Rubock MJ, Whitman M** 1996 A transcriptional partner for MAD proteins in TGF-β signalling. Nature 383:691–696
25. **Chen X, Weisberg E, Fridmacher V, Watanabe M, Naco G, Whitman M** 1997 Smad4 and FAST-1 in the assembly of activin-responsive factor. Nature 389:85–89
26. **Rodriguez C, Huang LJ, Son JK, McKee A, Xiao Z, Lodish HF** 2001 Functional cloning of the proto-oncogene brain factor-1 (BF-1) as a Smad-binding antagonist of transforming growth factor-β signaling. J Biol Chem 276:30224–30230
27. **Seoane J, Le HV, Shen L, Anderson SA, Massagué J** 2004 Integration of Smad and forkhead pathways in the control of neuroepithelial and glioblastoma cell proliferation. Cell 117:211–223
28. **Hadjantonakis AK, Gertsenstein M, Ikawa M, Okabe M, Nagy A** 1998 Non-invasive sexing of preimplantation stage mammalian embryos. Nat Genet 19:220–222
29. **Kananen K, Markkula M, Rainio E, Su JG, Hsueh AJ, Huhtaniemi IT** 1995 Gonadal tumorigenesis in transgenic mice bearing the mouse inhibin α-subunit promoter/simian virus T-antigen fusion gene: characterization of ovarian tumors and establishment of gonadotropin-responsive granulosa cell lines. Mol Endocrinol 9:616–627
30. **Svingen T, Spiller CM, Kashimada K, Harley VR, Koopman P** 2009 Identification of suitable normalizing genes for quantitative real-time RT-PCR analysis of gene expression in fetal mouse gonads. Sex Dev 3:194–204
31. **Wilhelm D, Hiramatsu R, Mizusaki H, Widjaja L, Combes AN, Kanai Y, Koopman P** 2007 SOX9 regulates prostaglandin D synthase gene transcription in vivo to ensure testis development. J Biol Chem 282:10553–10560
32. **Wilhelm D, Martinson F, Bradford S, Wilson MJ, Combes AN, Beverdam A, Bowles J, Mizusaki H, Koopman P** 2005 Sertoli cell differentiation is induced both cell-autonomously and through prostaglandin signaling during mammalian sex determination. Dev Biol 287:111–124
33. **Wilhelm D, Washburn LL, Truong V, Fellous M, Eicher EM, Koopman P** 2009 Antagonism of the testis- and ovary-determining pathways during ovotestis development in mice. Mech Dev 126:324–336
34. **Cocquet J, Pailhoux E, Jaubert F, Servel N, Xia X, Pannetier M, De Baere E, Messiaen L, Cotinot C, Fellous M, Veitia RA** 2002 Evolution and expression of FOXL2. J Med Genet 39:916–921
35. **Ottolenghi C, Pelosi E, Tran J, Colombino M, Douglass E, Nedorezov T, Cao A, Forabosco A, Schlessinger D** 2007 Loss of Wnt4 and Foxl2 leads to female-to-male sex reversal extending to germ cells. Hum Mol Genet 16:2795–2804
36. **Havelock JC, Rainey WE, Carr BR** 2004 Ovarian granulosa cell lines. Mol Cell Endocrinol 228:67–78
37. **Walsh DW, Godson C, Brazil DP, Martin F** 2010 Extracellular BMP-antagonist regulation in development and disease: tied up in knots. Trends Cell Biol 20:244–256
38. **Ottolenghi C, Uda M, Crisponi L, Omari S, Cao A, Forabosco A, Schlessinger D** 2007 Determination and stability of sex. Bioessays 29:15–25
39. **Yao HH** 2005 The pathway to femaleness: current knowledge on embryonic development of the ovary. Mol Cell Endocrinol 230:87–93

THYROID
Volume 21, Number 4, 2011

DOI: 10.1089/thy.2010.0005

A Study of the Etiology of Congenital Hypothyroidism in the Niigata Prefecture of Japan in Patients Born Between 1989 and 2005 and Evaluated at Ages 5–19

Keisuke Nagasaki,[1] Tadashi Asami,[2] Yohei Ogawa,[1] Toru Kikuchi,[1] and Makoto Uchiyama[1]

Background: The prevalence of congenital hypothyroidism (CH) increased during the period 1994–2002 in Japan. The reasons for these recently described increases in the prevalence of CH remain unclear. Moreover, the proportion of patients with different etiologies CH in the more recently diagnosed patients has not been established. In this study, we determined the etiologies of CH that were detected by neonatal screening in Niigata Prefecture, Japan.

Methods: A total of 100 patients having a diagnosis of CH (41 men and 59 women, aged 5–19 years old) were evaluated. To determine the etiology of CH, the patients underwent a ^{123}I thyroidal radioiodine uptake test, a scintigram, a saliva to plasma radioiodine ratio analysis, a perchlorate discharge test, thyroid ultrasonography, measurements of thyroidal function and thyroglobulin, and a thyrotropin (TSH)-releasing hormone tolerance test.

Results: Patients with overt CH ($n = 34$, elevated TSH levels with low free thyroxine levels) made up 34% of the total group, 56% of the patients had subclinical CH ($n = 56$, elevated TSH levels with normal free thyroxine levels), and 10% had normal thyroid function. These were patients who were considered to have transient hypothyroidism or hyperthyrotropinemia. Thyroid dysgenesis was the diagnosis in 73% of patients with overt CH, and the most of these had ectopic thyroid tissue. In contrast, thyroid dysgenesis was the diagnosis in only 36% of the patients with subclinical CH.

Conclusions: Only 50% of our patients with CH detected by neonatal screening had thyroid dysgenesis. With an increase in the percentage of patients with subclinical hypothyroidism, the prevalence of thyroid dyshormogenesis has increased. Studies of the frequency and etiology of CH should consider overt and subclinical CH separately.

Introduction

CONGENITAL HYPOTHYROIDISM (CH) is the one of the most common congenital endocrine disorders, occurring in about one in 3000–4000 live births (1). The majority of cases (75%–85%), based on using a thyrotropin (TSH) cutoff values of 20 mIU/L in a dry blood spot, have been reported to be due to thyroid dysgenesis; the remaining were caused by various types of thyroid dyshormogenesis (1,2). Recently, Corbetta *et al.* (3), in a study of patients with CH who were born between 1999 and 2005 in Italy, noted a prevalence of CH of one in 1446. In this study, a blood TSH concentration of greater than 10 or 12 mU/L was the criteria used to screen for CH. In contrast to the earlier studies, in the Corbetta *et al.* study (3), 32% of infants with CH had thyroid dysgenesis and the remaining had thyroid dyshormogenesis.

Neonatal screening for CH was initiated in Japan in 1979. Since then, almost all newborns have been tested for CH in Japan. In 1989, a highly sensitive method for detecting CH was introduced, and by 1992, an enzyme-linked immunosorbent assay had completely replaced older methods such as radioimmunoassay and enzyme immunoassay. During the period 1994–2002, the incidence and prevalence for CH in Japan had an upward trend despite the fact that the criteria for the diagnosis of CH, and screening methods including the TSH assay, did not change (4). A report published in 2004 suggested prenatal iodine exposure as a possible reason for this trend (5) but this, or other reasons for the trend, have not been established.

[1]Division of Pediatrics, Department of Homeostatic Regulation and Development, Niigata University Graduate School of Medicine and Dental Sciences, Niigata, Japan.
[2]Department of Nursing, Faculty of Nursing, Social Welfare, and Psychology, Niigata Seiryo University, Niigata, Japan.

It is also not known what etiologies accounted for CH in patients born from about 1994 to recent years.

In the present study, we sought to determine the etiology of CH in patients born between 1989 and 2005 in Japan, using the Niigata prefecture of Japan as our sampling area.

Methods

Between April 1989 and March 2006, 437,867 newborns were screened for CH in Niigata prefecture. Blood samples were collected on filter paper within the first 4–7 postnatal days. TSH was determined in single 0.3 cm disks punched from the filter paper blood. TSH was measured in the filter paper sample using an enzyme-linked immunosorbent assay (TSH: Enzaplate N-TSH; Bayer Co.). Detection limits were 0.5 mU/L for TSH. All CH screening tests are centralized in the Niigata Health Laboratory center.

In the Niigata prefecture, a blood TSH cutoff level of 8 mU/L was established for the initial neonatal screen when the program was started in 1982. When the initial blood TSH was between 8 and 30 mU/L, a second specimen was reevaluated at Niigata Health Laboratory center. If that specimen was also greater than 8 mU/L, the policy was that a confirmatory test be run within 30 days at the patient's medical institution. If the initial blood TSH was in excess of 30 mU/L, the policy was that a confirmatory test be run within 14 days at the patient's medical institution. The tests that were run at the patient's medical institution in addition to repeating the TSH was a thyroxine (T4) or free T4 (FT4) and free triiodothyronine (FT3). In addition, thyroid morphology was evaluated by ultrasonography in almost all patients. Neonates with persistent serum TSH values over than 10 mU/L and normal or low FT4 were considered to have CH, and treatment was generally started. Neonates with serum TSH values less than 10 mU/L were considered to have normal thyroid function.

Among the 437,867 newborns who were screened, 367 were considered positive for CH and were referred to pediatric endocrinologists. Of these, 333 (91%) were seem at our institution, 240 of whom were started on oral levothyroxine therapy for CH. Of the remaining patients, 86 had normal thyroid function and 7 had a chromosomal abnormality. Most patients with CH were reevaluated at 2 years of age to see whether they continued to need levothyroxine. If their serum TSH was less than 5 mU/L while off thyroid hormone replacement for 4 weeks, they were considered to have had transient CH or hyperthyrotropinemia. Of the 240 patients who had been started on levothyroxine during infancy, 12 were lost to followup, 57 were diagnosed as having transient CH or transient hyperthyrotropinemia, and in 171 the diagnosis of CH was confirmed. These latter 171 patients were the ones eligible for our study of the etiology of CH. Among these 171 patients with CH, 100 patients (58% of the eligible patients, 41 boys and 59 girls) actually participated in the study. Most of the 71 patients who did not participate could not take a capsule orally or remain in the supine position for the duration of a radioiodine uptake (RAIU) test. The 100 patients who participated were born between 1989 and 2005 and ranged in age from 5 to 19 (5–9 years old; $n = 53$, 10–14 years old; $n = 33$, 15–19 years old; $n = 14$) at the time of the study of the current status of their diagnosis of CH, which was based on earlier screening guidelines for CH (6). Studies were performed between April 2004 and March 2008.

Protocol for determination of etiology of CH

Levothyroxine treatment was stopped at the beginning of the study and T3 was started in three daily doses, the total of which was 25% by weight of the levothyroxine dose the patient had been on. This was given for 3 weeks. After this, there was a 7-day period during which no thyroid hormone was administered and then a ^{123}I thyroidal RAIU, saliva to plasma radioiodine ratio, perchlorate discharge test (if the RAIU was 20% or more), scintigram, thyroid ultrasonography, and measurements of serum TSH, FT4, FT3, T3, T4, and thyroglobulin were performed. A thyrotropin-releasing hormone (TRH) stimulation test (7 μg/kg intravenous Protirelin®, HIRTONIN; Takeda Pharmaceuticals Ltd.) was also performed. Blood samples were drawn at 0, 30, 60, 90, and 120 minutes for TSH, and at 0 and 120 minutes for T3, and FT3. The T3 and FT3 increments after the TRH test (ΔT3, ΔFT3) were compared with normal values (ΔT3>25 ng/dL, ΔFT3>0.6 pg/mL) (7,8). FT3, FT4, and TSH were determined by chemiluminescent enzyme immunoassays (E-test Tosoh II kit; Tosoh Corporation). Normal ranges in our laboratory are FT3 = 2.1 to 4.6 pg/mL, FT4 = 0.9 to 1.6 ng/dL, TSH = 0.6 to 4.2 mU/L, and peak TSH levels during the TRH test are <30 mU/L. Thyroid ultrasonography was performed with LOGIQ S6 (GE health care) equipment with high-frequency probes (10 MHz). The maximum thickness and maximum width of the bilateral lobes were measured by transverse scans. The sum of thickness and the sum of width were used to estimate thyroid gland size, as a function of height (9). Thyroid hypoplasia and hyperplasia were defined as values lower than −1.0 SD and higher than +1 SD from the normal mean, respectively.

Based on thyroid ultrasonography and scintigraphy, patients with CH were classified as having thyroid agenesis, ectopy, hemiagenesis, hypoplasia, a normal-size thyroid, or hyperplasia according to thyroid morphology. Patients with thyroid hyperplasia were classified as having dyshormogenesis and were sub-classified as follows. If their saliva to plasma radioiodine ratio was 10 or less, they were considered to have an iodine concentration defect. If the perchlorate discharge test was more than 20%, they were considered to have a complete iodide organification defect, and if it was 10%–20%, they were considered to have a partial organification defect. If the serum thyroglobulin concentration was low (thyroglobulin <10 ng/mL), they were considered to have a thyroglobulin synthesis defect. Patients with thyroid hyperplasia who did not have any of these conditions were considered to have a post iodide organification defect in thyroid hormone synthesis. Among patients who had normal thyroid glands, patients who had a less than normal T3 or FT3 response to TRH were considered to have resistance to TSH (RTSH) and were classified as having dyshormonogenesis. All of the patients in this classification had a TSH response to TRH. Those in the normal thyroid size group who did not have RTSH were considered to be "idiopathic." Thyroid agenesis, ectopy, hemiagenesis, and hypoplasia were categorized as thyroid dysgenesis.

All 100 patients who enrolled in the study had, as previously noted, a previous history and tests that supported the diagnosis of CH. Nonetheless, not all patients who were evaluated by the study protocol had overt or even subclinical hypothyroidism (see Results). On the basis of the study

TABLE 1. RESULTS OF THE ETIOLOGY OF CONGENITAL HYPOTHYROIDISM

	Subclinical hypothyroid group n = *56*	*OH group* n = *34*	*total*	*TH group* n = *10*
Thyroid dysgenesis	20/56 (35.7%)	25/34 (73.5%)	45/90 (50%)	
Agenesis	0	3		
Ectopy	1	21		
Hypoplasia	17	1		
Hemiagenesis	2	0		
Thyroid dyshormogenesis	36/56 (64.3%)	8/34 (23.5%)	45/90 (50%)	
Iodine concentration defect	0	0		
Iodine organification defect	1	1		
Thyroglobulin synthesis defect	0	0		
Defect in thyroid hormone synthesis after iodine organic	0	2		
Idiopathic	27	1		
Resistance to thyrotropin	8	4		
Others*	0	1		

*Coexistence of Hashimoto disease.

protocol results, patients were divided into three groups based on their serum TSH and thyroid hormone levels after they had been off thyroid hormone for one week. Patients who had elevated basal TSH levels or whose serum TSH increased to 30 mU/L or higher during the during TRH test but who had normal serum FT4 concentrations were assigned to the subclinical hypothyroid (SCH) group. Patients who had elevated serum TSH concentrations and low serum FT4 concentrations were assigned to the overt hypothyroid (OH) group. Patients who had normal serum TSH and FT4 concentrations were assigned to the transient hypothyroid (TH) group.

The study was approved by the Institutional Review Board Committee at Niigata University School of Medicine, and informed consent was given by all participants in this study or by their parents or guardians on their behalf.

Results

In all patients, peak serum TSH levels were found 30 minutes after TRH administration and declined thereafter. The etiologies of CH in the study patients are shown in Table 1 and Figure 1. The OH group made up 34% of the patients with CH, the SCH group made up comprised 56% of the patients with CH, and the TH group comprised 10% of the patients with CH. The distribution of FT4 and TSH values in the three groups are shown in Figure 2. Thyroid dysgenesis accounted for 73.4% of the OH group, and almost all had thyroid ectopy. In contrast, thyroid dysgenesis accounted for 35.7% of the SCH group, and half of the SCH group had normal thyroid position and size without typical thyroid dyshormogenesis and were classified as idiopathic.

Among patients with SCH, almost all patients except one had a normally located thyroid gland. Clinical RTSH was detected in 12 patients and was found in both patients with OH and those with SCH.

Discussion

This was the study of the etiologies of CH as detected by neonatal screening in Japan. In 10 of the 100 study patients who carried a diagnosis of CH, this diagnosis could not be confirmed. Of the remaining 90 patients, 45 (50%) had thyroid dysgenesis, and 45 (50%) had thyroid dyshormogenesis patients. This contrasts with earlier findings that the majority of CH cases (about 75%–85%), had some form of thyroid dysgenesis, including agenesis, ectopy, hemiagenesis, or hypoplasia (1,2) with the remaining patients having thyroid dyshormogenesis. These epidemiological and clinical classifications, however, were based on screening programs with TSH cutoff values of 20–40 mU/L or first performing T4 screening with backup TSH measurements in the dried blood spot. In contrast, our initial screen was based on a TSH cutoff value of 8 mU/L, which likely detected more of the milder forms of CH. These were mostly subclinical hypothyroidism. We classified patients in whom the diagnosis of CH was confirmed by the study as SCH or OH. About 73% of the OH patients with OH had thyroid dysgenesis in agreement with earlier reports (1,2); approximately 90% of those were ectopic.

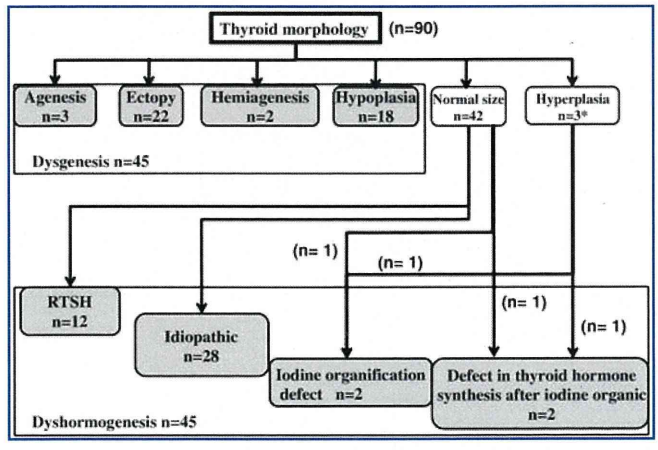

FIG. 1. Classification of the etiology of congenital hypothyroidism. *n* shows the number of patients with congenital hypothyroidism. Among normal sizes, cases of less than normal value ΔT3 and ΔFT3 on thyrotropin-releasing hormone tests are classified as clinical resistance to thyrotropin (RTSH). Normal sizes without RTSH or typical dyshormogenesis were classified as "idiopathic." *One patient had coexistence of Hashimoto disease.

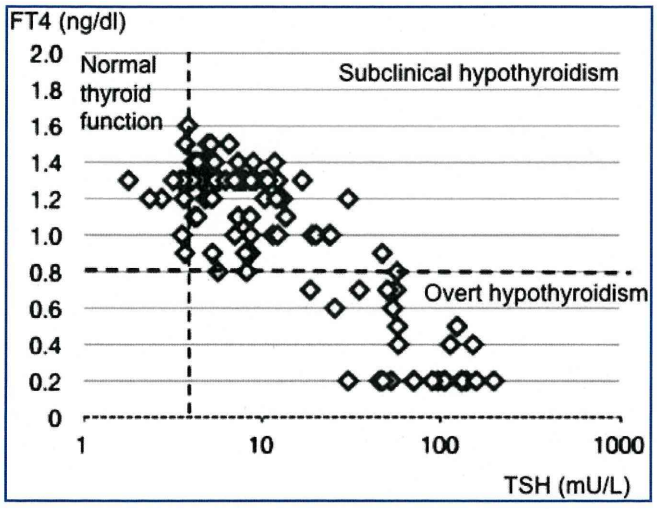

FIG. 2. The distribution of free thyroxine (FT4) and TSH values in the three groups after the withdrawal of replacement in this study.

In contrast, only 36% of the SCH group had thyroid dysgenesis. In future studies, we recommend that OH and SCH forms of CH be considered separately, but followup studies of patients initially screened using relatively high blood spot TSH concentrations may be relatively underrepresented by patients with SCH.

RTSH was detected in 12 patients who were in both the SCH and OH groups. RTSH is a heterogeneous condition where there is a variable degree of insensitivity to biologically active TSH. In this study, we defined clinical RTSH based on the incremental increase in serum FT3 after TRH administration. A similar approach was taken by Balavoine *et al.* (10). Unfortunately, there is very little definitive reference data for TRH stimulation tests, and TRH is no longer marketed in many regions. RTSH is classically caused by loss-of-function mutations of the TSH receptor gene (*TSHR*), but some patients exhibit a RTSH-like phenotype in the apparent absence of *TSHR* mutations. Some have mutations of *PAX8*, *GNAS1*, or *TITF1* (11). Patients with mutations of *TSHR* have a broad clinical spectrum, depending on the degree of TSH unresponsiveness, ranging from subclinical to overt hypothyroidism (12). Some patients have hypoplastic thyroid glands; in others, thyroid size is normal. A more accurate etiologic study would require an active genetic analysis in addition to a conventional etiology of CH.

Almost half of our patients in the SCH group were classified as "idiopathic" on the basis of normal baseline FT4, elevated TSH levels, a normal T3 response to TRH, and normal thyroid images. Many pediatric endocrinologists do not consider patients of this type to necessarily have permanent hypothyroidism (13). This category includes various conditions such as mild dyshormogenesis, a thyroid gland in the lower limits of normal size, and mild resistance to TSH,. These are classified as dyshormogenesis according to conventional classification, as they all have a normal thyroid gland position. Further studies to define more accurately the underlying pathophysiology in these patients and whether they are longstanding are needed.

In summary, in our study of Japanese children and teenagers who carried a diagnosis of CH that was made in conjunction with a screening program with a relatively low initial TSH cutoff value, the diagnosis of CH could not be confirmed in 10% of the patients. In the remaining 90%, only 50% of these had thyroid dysgenesis and there was a relatively high proportion of those who would be judged to have subclinical hypothyroidism, at least using criteria developed in adults. Further followup studies of CH should consider both subclinical and overt hypothyroidism. In addition, the screening strategies of the various neonatal programs should be scrutinized regarding the possibility that some employ TSH cutoff values that are not sufficiently sensitive.

Disclosure Statement

The authors declare that no competing financial interests exist.

References

1. Fisher DA, Grueters A 2008 Disorder of the thyroid in the newborn and infant. In: Sperling MA (ed) Pediatric Endocrinology, third edition. Saunders Elsevier, Philadelphia, pp 206–217.
2. Fisher DA 1983 Second International Conference on Neonatal Thyroid Screening: progress report. J Pediatr **102:**653–654.
3. Corbetta C, Weber G, Cortinovis F, Calebiro D, Passoni A, Vigone MC, Beck-Peccoz P, Chiumello G, Persani L 2009 A 7-year experience with low blood TSH cutoff levels for neonatal screening reveals an unsuspected frequency of congenital hypothyroidism (CH). Clin Endocrinol **71:** 739–745.
4. Gu YH, Kato T, Harada S, Inomata H, Aoki K 2010 Time trend and geographic distribution of treated patients with congenital hypothyroidism relative to the number of available endocrinologists in Japan. J Pediatr **157:**153–157.
5. Nishiyama S, Mikeda T, Okada T, Nakamura K, Kotani T, Hishinuma A 2004 Transient hypothyroidism or persistent hyperthyrotropinemia in neonates born to mother with excessive iodide intake. Thyroid **14:**1077–1083.
6. Inomata H, Matsuura N, Tachibana K, Kusuda S, Fukushi M, Umehashi H, Suwa S, Niimi H, Fujieda K 1999 Guideline for neonatal mass-screening for congenital hypothyroidism. Clin Pediatr Endocrinol **8:**51–55.
7. Harada S, Matsuura N, Keiko S 2004 Report of Health Labour Sciences Research Grants (Research on Child and Families): research on efficient execution of mass screening.; Draft of consensus guideline for mild congenital hypothyroidism, pp 43–47 (In Japanese). http://mhlw-grants.niph.go.jp/niph/search/NIDD00.do.
8. Vogt P, Girard J, Staub JJ 1978 Thyroid-stimulating hormone (tsh), triiodothyronine (t3) and thyroxine (t4) response to intravenous and oral stimulation with synthetic thyrotropin-releasing hormone (trh) in young healthy adults. Klin Wochenschr **56:**31–35.
9. Ueda D, Mitamura R, Suzuki N, Yano K, Okuno A 1992 Sonographic imaging of the thyroid gland in congenital hypothyroidism. Pediatr Radiol **22:**102–105.
10. Balavoine AS, Ladsous M, Velayoudom FL, Vlaeminck V, Cardot-Bauters C, d'Herbomez M, Wemeau JL 2008 Hypothyroidism in patients with pseudohypoparathyroidism type Ia: clinical evidence of resistance to TSH and TRH. Eur J Endocrinol **159:**431–437.

11. Nagasaki K, Narumi S, Asami T, Kikuchi T, Hasegawa T, Uchiyama M 2008 Mutation of a gene for thyroid transcription factor-1 (TITF1) in a patient with clinical features of resistance to thyrotropin. Endocr J **55**:875–878.
12. Narumi S, Muroya K, Abe Y, Yasui M, Asakura Y, Adachi M, Hasegawa T 2009 TSHR mutations as a cause of congenital hypothyroidism in Japan: a population-based genetic epidemiology study. J Clin Endocrinol Metab **94**:1317–1323.
13. Eugster EA, LeMay D, Zerin JM, Pescovitz OH 2004 Definitive diagnosis in children with congenital hypothyroidism. J Pediatr **144**:643–647.

Address correspondence to:
Keisuke Nagasaki, M.D., Ph.D.
Division of Pediatrics
Department of Homeostatic Regulation and Development
Niigata University Graduate School of Medicine and Dental Sciences
1-757, Asahimachi, Niigata 951-8510
Japan

E-mail: nagasaki@med.niigata-u.ac.jp

Endocrinology. First published ahead of print April 23, 2012 as doi:10.1210/en.2011-1627

A Genome-Wide Expression Profile of Adrenocortical Cells in Knockout Mice Lacking Steroidogenic Acute Regulatory Protein

Tomohiro Ishii, Toshikatsu Mitsui, Sadafumi Suzuki, Yumi Matsuzaki, and Tomonobu Hasegawa

Departments of Pediatrics and Physiology, School of Medicine, Keio University, Tokyo 160-8582, Japan

Steroidogenic acute regulatory protein (StAR) facilitates cholesterol transfer into the inner mitochondrial membrane in the acute phase of steroidogenesis. Mice lacking StAR (*Star*$^{-/-}$) share phenotypes with human individuals having congenital lipoid adrenal hyperplasia including compromised production of steroid hormones and florid accumulation of cholesterol esters in adrenal glands and gonads. To define a specific pattern of molecular changes with StAR deficiency, we performed transcriptome analysis of adrenal cells selectively isolated by fluorescent-activated cell sorting at embryonic d 17.5 or 18.5 in seven wild-type (*Star*$^{+/+}$) or four *Star*$^{-/-}$ mice having the transgene targeting the enhanced green fluorescent protein to cell lineages that express StAR. A gene expression profile was obtained by whole-mouse genome microarray and confirmed by quantitative real-time PCR, identifying 1206 and 767 significantly up-regulated and down-regulated genes, respectively, in *Star*$^{-/-}$ mice compared with *Star*$^{+/+}$ mice (fold difference ≥ 2 and P value < 0.05 with false discovery rate < 0.2). In *Star*$^{-/-}$ mice, expression levels of genes involved in cholesterol efflux and the inflammatory response were significantly up-regulated, whereas those related to steroid hormone biosynthesis or cholesterol biosynthesis and influx were not significantly changed. Immunoreactive Iba1 or F4/80 (macrophage marker) in adrenal glands of *Star*$^{-/-}$ mice was detected not only in an increased number of resident macrophages but also in most adrenocortical cells. These findings expand our understanding of the pathophysiology of adrenal glands with the disruption of StAR and propose a reciprocal interaction between adrenocortical cells and resident macrophages inside adrenal glands of *Star*$^{-/-}$ mice. (***Endocrinology* 153: 0000–0000, 2012**)

Steroidogenic acute regulatory protein (StAR) is one of the mitochondrial proteins under complex transcriptional control that is localized at crista facing the inner mitochondrial membrane or at the intermembrane space in steroidogenic cells, based on immunohistochemistry and electron microscopy (1, 2). StAR functions on the cytoplasmic aspect of the outer mitochondrial membrane, facilitates translocation of cholesterol from the outer to the inner mitochondrial membrane when newly synthesized, and regulates the rate-limiting step of steroidogenesis (3–7). Both humans having *STAR* mutations [congenital lipoid adrenal hyperplasia (lipoid CAH)] and knockout mice lacking StAR (*Star*$^{-/-}$ mice) show significant defects in steroid hormone biosynthesis and diffuse accumulation of lipid droplets in the steroidogenic cells of the adrenal glands and gonads (8–11). It has been well described that the onset of steroid hormone deficiency is variable among the adrenal cortex, testis, and ovary, leading to a two-hit model for the pathogenesis of lipoid CAH (8). This model proposes that the ultimately accumulated cholesterol esters abrogate the residual capacity of the StAR-independent steroidogenesis that are initially preserved in StAR-deficient steroidogenic cells. However, the molecular mechanism behind the pathophysiology of steroidogenic cells in StAR deficiency remains to be clarified.

ISSN Print 0013-7227 ISSN Online 1945-7170
Printed in U.S.A.

doi: 10.1210/en.2011-1627 Received August 14, 2011. Accepted March 28, 2012.

Abbreviations: BAC, Bacterial artificial chromosome; E, embryonic day; eGFP, enhanced green fluorescent protein; FAC, fluorescent-activated cell (sorting); IPA, Ingenuity Pathways Analysis; lipoid CAH, congenital lipoid adrenal hyperplasia; LXR, liver X receptor; Mc2r, melanocortin type 2 receptor; qPCR, quantitative real-time PCR; SF-1, steroidogenic factor-1; Shh, sonic hedgehog; StAR, steroidogenic acute regulatory protein; Tlr2, toll-like receptor-2; Wnt4, wingless-related mouse mammary tumor virus integration site 4.

To delineate the molecular mechanism of cholesterol transport by StAR into the inner mitochondrial membrane, we have previously performed *in vivo* studies using bacterial artificial chromosome (BAC) transgenesis (11). We targeted expression of either wild-type StAR or mutant StAR lacking its mitochondrial targeting signal in $Star^{-/-}$ mice, confirming the ability of StAR lacking the mitochondrial targeting signal to perform some essential functions but also demonstrating the important functional defects in adrenal glands and gonads (11). This observation still needs confirmation because it differs from previous *in vitro* studies (6, 12). Further to this, we created transgenic mice carrying a BAC transgene targeting enhanced green fluorescent protein (eGFP) to steroidogenic cells of the adrenal cortex and gonads under the control of all regulatory *cis* sequences of the *Star* gene (StAR/eGFP mice). The StAR/eGFP mice provided a useful strategy for selectively isolating steroidogenic cells that normally express StAR.

To define a specific pattern of global changes in gene expression with the disruption of StAR, we performed transcriptome analysis of putative steroidogenic cells in adrenal glands of $Star^{-/-}$ mice and deciphered gene ontogeny or biological pathways that could explain the pathophysiology of StAR deficiency. The present study identified significant changes of gene expression associated with cholesterol efflux and inflammatory response in adrenocortical cells, proposing the first evidence for a reciprocal interaction between adrenocortical cells and resident macrophages inside adrenal glands with disruption of StAR.

Materials and Methods

Experimental animals

All experiments involving mice were approved by the Laboratory Animals Center at School of Medicine, Keio University (Tokyo, Japan). We collected $Star^{+/+}$ or $Star^{-/-}$ embryos carrying the transgene expressing eGFP under the control of the endogenous *Star* regulatory sequences. As reported in our previous study (11), the transgene was created by insertion of eGFP cDNA into the coding region of *Star* in a bacterial artificial chromosome clone containing the *Star* gene with 47 kb of 5′- and 62 kb of 3′-flanking regions of the gene (StAR/eGFP BAC) and was proved to target eGFP reporter expression to steroidogenic cells in adrenal cortex, testis, and ovary of adult mice driven by *Star* endogenous promoter. Mice were genotyped by PCR assays using the primer sets detailed below. *Star* genotype was determined using a forward primer (ATGATGCACAGCCTTCCACGG), a reverse primer no. 1 (CCATCACTGGCAGAAGCTCAGA), and a reverse primer no. 2 (ATCTCGTCGTGACCCATGGC). Chromosomal sex was determined by the presence or absence of *Sry* gene using a forward primer (AAGCGCCCCATGAATGCATT) and a reverse primer (CGATGAGGCTGATATTTATA). The presence of the StAR-eGFP BAC transgene was examined using a forward primer (AGCTGAAGCCATATTGGGGAACAAG) and a reverse primer (AGTGAATTGTAATACGACTCACTATAGGGC). In compliance with ethical recommendations, all embryos were collected from pregnant female mice fully anesthetized with an intraabdominal injection of pentobarbital.

Cell sorting

We selectively purified steroidogenic cells from adrenal glands at embryonic day (E) 17.5 or 18.5 in $Star^{+/+}$ (n = 7) or $Star^{-/-}$ mice (n = 4) with the StAR/eGFP BAC transgene. Adrenal glands were dissected out from the embryos and single cell suspensions were prepared by enzymatic dissociation in PBS containing 0.125% trypsin, 0.5% EDTA, and 5% deoxyribonuclease I type IV (Sigma-Aldrich Corp., St. Louis, MO) for 30–60 min at 37 C with gentle shaking. Cells were spun down and resuspended in ice-cold PBS containing 3% fetal calf serum and passed through 40-μm cell strainers (Falcon BD Biosciences, Becton Dickinson, Franklin Lakes, NJ). eGFP-positive cells were selectively isolated by fluorescent-activated cell (FAC) sorting (Vantage SE; Becton Dickinson).

RNA preparation

Total RNA was isolated from FAC-sorted cell populations with TRIzol reagent (Invitrogen Corp., Carlsbad, CA) and the subsequent NucleoSpin RNA XS (Macherey-Nagel GmbH and Co. KG, Duren, Germany). RNA was quantified using a Nanodrop ND1000 spectrophotometer (Nanodrop Technologies, Wilmington, DE). RNA quality and integrity was assessed using an Agilent 2100 bioanalyzer (Agilent Technologies, Inc., Palo Alto, CA).

mRNA was linearly amplified from 1.0 ng total RNA from each mouse by MessageAmp II aRNA amplification kit (Applied Biosystems/Ambion, Austin, TX). In brief, double-stranded cDNA was synthesized with an oligo-dT primer bearing a T7 promoter using ArrayScript reverse transcriptase, and was used as a template for *in vitro* transcription with T7 RNA polymerase to generate multiple copies of amplified mRNA. Amplified mRNA was purified using an RNAeasy column (QIAGEN, Valencia, CA). 200 ng of mRNA was reverse transcribed to generate double-stranded cDNA templates for cRNA probes for microarray analysis by SuperScript II RT (Invitrogen Corp.) with oligodeoxythymidine primers.

Microarray analysis

The transcription profile was determined by microarray analysis with Cy3-labeled cRNA using one-color Quick Amp labeling kit (Agilent Technologies). Dye incorporation and cRNA yield was checked with a Nanodrop ND1000 spectrophotometer (Nanodrop Technologies). Cy3-labeled cRNA was hybridized to a whole-mouse genome microarray G4122F (Agilent Technologies). This array platform is comprised of 41,534 probes of 60-mer oligonucleotides, representing more than 41,000 transcripts of mouse genome (http://www.agilent.com). The hybridized chips were scanned with a gene array scanner (Agilent Technologies) at the Core Instrumentation Facility, School of Medicine, Keio University (Tokyo, Japan). The observed data were analyzed using Gene Spring GX 11.5.1 (Agilent Technologies). The raw expression values were normalized to

the 75th percentile in all samples, and the data from very low signal values (less than the 20th percentile) were removed. The difference in gene expression was assessed by averaging the normalized values and performing a pairwise analysis between $Star^{+/+}$ mice and $Star^{-/-}$ mice. Differentially expressed genes were defined as having a difference in a gene expression ratio of 2-fold or greater and a P value using a Student t test of less than 0.05 with a false discovery rate (Q value) of Benjamin and Hochberg (13) of less than 0.2, according to recommendations by the MicroArray Quality control (14, 15).

Furthermore, gene ontogeny and biological pathway analyses for the differentially expressed genes were performed through Ingenuity Pathways Analysis (IPA) version 9 (Ingenuity Systems, Inc., Redwood City, CA) and NextBio (https://www.nextbio-.com, Cupertino, CA). The IPA revealed the canonical pathways most significantly relevant to the data set of the microarray analysis by right- or two-tailed Fisher's exact probability test. NextBio identified a list of biogroups or cell types most significantly correlated with the differentially expressed genes based on the information of available 967 RNA expression studies with 318 mouse cell types (as of October 22, 2011) (16). A correlation score represents magnitude of correlation between gene expression profiles, computed with the running Fisher algorithm, a nonparametric rank-based statistical approach. A P value was determined by Fisher's exact probability test with multiple comparison test.

Quantitative real-time PCR (qPCR)

The expression levels for genes of interest were validated by qPCR with additional samples of FAC-sorted cells from adrenal glands of $Star^{+/+}$ (n = 3) or $Star^{-/-}$ males (n = 4) at E17.5 or 18.5. Total RNA was isolated and mRNA was amplified by the same methods as the microarray analysis. Two hundred forty nanograms of mRNA were reverse transcribed using SuperScript II RT (Invitrogen) with oligo-deoxythymidine primers. qPCR reactions were performed in 10-μl volumes containing cDNA synthesized from 0.5 ng mRNA by the intercalater method using SYBR Premix Ex Taq II (Takara Bio Inc., Otsu, Japan) and ABI Prism 7500 Fast (PE Applied Biosystems, Foster City, CA). Primer pairs were purchased from Takara Bio Inc., except for primers for *Cyp11a1* (17). The reaction conditions were 3 min at 95 C and 40 cycles of 15 sec at 95 C and 1 min at 60 C. The relative quantity of gene expression was calculated using the delta delta cycle threshold method. The average dCt of $Star^{+/+}$ mice was determined as a calibrator. *Gapdh* was chosen as an endogenous control for normalization of each gene studied, based on a step-wise comparison method with other housekeeping genes including *Ras18*, *Ywhaz*, *Tbp*, and *Hprt1* (18). Amplification of specific transcripts was confirmed by melting curve profiles at the end of each PCR. qPCR data were analyzed using 7500 Software version 2.0 (PE Applied Biosystems). Statistical difference in gene expression levels between $Star^{+/+}$ and $Star^{-/-}$ mice was examined using a Student t test, with $P < 0.05$ considered significant. A comparison of the fold changes of gene expression level between the microarray and the qPCR was analyzed using the Bland-Altman method (19) (MedCalc Software, Mariakerke, Belgium), with $P < 0.05$ considered significant.

Immunohistochemistry

Immunohistochemical analysis was performed on frozen tissues for eGFP or on fixed whole embryos for macrophage markers or steroidogenic factor-1 (SF-1; Nr5a1). For eGFP analysis, adrenal glands or gonads were harvested from each embryo at E17.5 and 18.5, embedded in Tissue Tek (Sakura, Tokyo, Japan), and stored at −80 C. The cryosections of the adrenal glands and the gonads were fixed by 4% paraformaldehyde in PBS for 10 min at room temperature. For analysis of the macrophage markers and SF-1, whole embryos were directly fixed by Tissue Fixative (Genostaff Co., Ltd., Tokyo, Japan) for 2 d at room temperature. Embryo sections containing adrenal glands were treated with proteinase K. For both preparations, endogenous peroxidase was blocked with 0.3% hydrogen peroxide in methanol for 30 min, followed by incubation with protein block (Dako, Glostrup, Denmark) and avidin/biotin blocking kit (Vector laboratories, Burlingame, CA). The sections were incubated with either rabbit antigreen fluorescent protein polyclonal antibodies (Molecular Probes, Eugene, OR), monoclonal antibody against macrophages (F4/80 antigen) (Acris Antibodies GmbH, Herford, Germany), rabbit anti-Iba1 polyclonal antibodies (Wako Pure Chemical Industries, Ltd., Osaka, Japan), or monoclonal antibody against SF-1 (TransGenic, Inc., Kobe, Japan) at 4 C overnight. After washing with Tris-buffered saline, they were incubated with biotin-conjugated immunoglobulin for 30 min at room temperature, followed by the addition of peroxidase-conjugated streptavidin (Nichirei Biosciences Inc., Tokyo, Japan) for 5 min. Peroxidase activity was visualized by diaminobenzidine. The sections were counterstained with Mayer's hematoxylin (Muto Pure Chemical Co., Ltd., Tokyo, Japan), dehydrated, and then mounted with Malinol (Muto).

Results

eGFP expression in adrenal glands of StAR/eGFP transgenic mice at E17.5 and 18.5

To isolate steroidogenic cells from adrenal glands, we used transgenic mice carrying the StAR/eGFP BAC transgene, which drives eGFP expression under control of the endogenous *Star* promoter. It has been reported that StAR is specifically expressed in steroidogenic cells such as adrenocortical cells, Leydig cells, theca cells, neurons, and glial cells (7). To confirm which cell lineages express eGFP within adrenal glands or testes, we examined intrinsic fluorescence of eGFP (data not shown) and immunoreactivity against eGFP antibodies with embryos carrying the StAR/eGFP BAC transgene at E17.5 and 18.5. As shown in Fig. 1, eGFP expression was identified in the adrenal cortex and in the interstitial region of the testis in $Star^{+/+}$ or $Star^{-/-}$ mice having the transgene, consistent with the location of adrenocortical and Leydig cells. No eGFP expression was determined in the fetal ovaries. At this developmental stage, eGFP expression was comparable in the adrenal cortex of male and female embryos. Overall, the StAR/eGFP BAC transgene targets eGFP to endoge-

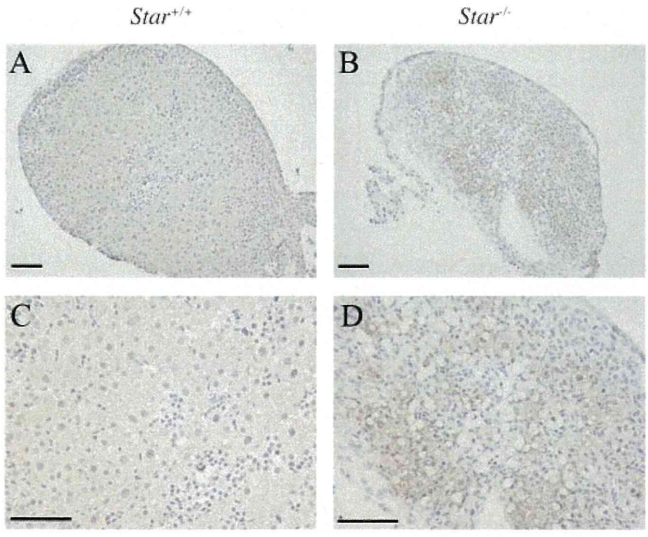

FIG. 1. Expression of Star/eGFP BAC transgene in adrenal glands of $Star^{+/+}$ or $Star^{-/-}$ mice at E17.5–18.5 by immunohistochemistry. A and C, $Star^{+/+}$. B and D, $Star^{-/-}$. C and D show higher magnification of A and B, respectively. *Scale bars*, 100 μm.

nous steroidogenic cells in adrenal glands and testes at E17.5 and 18.5, as we previously reported in adult mice.

Microarray analysis

To define specific changes associated with StAR deficiency, we performed transcriptome analysis with sorted eGFP-positive cells in adrenal glands of $Star^{+/+}$ or $Star^{-/-}$ embryos and identified a total of 1973 differentially expressed genes between them (Supplemental Table 1 and 2 published on The Endocrine Society's Journals Online web site at http://endo.endojournals.org). All original microarray data described in this study were submitted on a public database, National Center for Biotechnology Information's Gene Expression Omnibus (http://www.ncbi.nlm.nih.gov/geo) and is accessible through Gene Expression Omnibus series accession number GSE31328. Of 1973 differentially expressed genes, 1206 and 767 genes were significantly up-regulated and down-regulated, respectively, in adrenal steroidogenic cells derived from $Star^{-/-}$ mice compared with those from $Star^{+/+}$ mice (Supplemental Tables 1 and 2). No significant difference was found in expression of genes related to steroid hormone biosynthesis or cholesterol biosynthesis and influx, except for StAR. In contrast, genes related to cholesterol efflux such as those for liver X receptors (LXR) and ATP-binding cassettes were significant up-regulated. Adrenal glands at this stage also contain two different cell lineages, an adult zone in the outer cortices and a fetal zone in the inner cortices (20, 21). We found a significant decrease in expression of genes involved in the development of adrenocortical progenitor cells.

We performed further gene ontology and biological pathway analysis of the 1973 differentially expressed genes by using the IPA and the Nextbio and revealed the canonical pathways and biological functions to which differentially expressed genes were most significantly relevant. The IPA analysis unexpectedly revealed a significant association between the differentially expressed genes and the canonical pathways of inflammatory or immune response including dendritic cell maturation ($P = 2.1 \times 10^{-10}$), the antigen presentation pathway (1.4×10^{-9}), allograft rejection signaling (1.6×10^{-8}), the communication between innate and adaptive immune cells (1.0×10^{-7}), and IL-4 signaling (2.0×10^{-6}). Consistent with these data, the NextBio identified the immune response (correlation score 132.50, $P = 2.9 \times 10^{-58}$) as the most significant biogroup and the macrophage of the peripheral tissue of C57BL/6 (263.9, 2.5×10^{-115}), the microglial cell of C57BL/6 (255.8, 7.8×10^{-112}), and the dendritic cell follicular of lymph node of BALB/cAnNCrlCrlj (239.0, $1.6.8 \times 10^{-104}$) as the most significant cell types positively correlated with the differentially expressed genes. In fact, the genes related to the inflammatory or immune response were significantly up-regulated in the $Star^{-/-}$ mice.

Quantitative PCR

To verify the results of the microarray analysis, we determined gene expression levels of different samples by qPCR. We focused on genes of interest related to differentiation of adrenal glands, steroidogenesis, or cholesterol trafficking. The Bland-Altman plot analysis showed no statistically significant difference in fold changes of expression level of those genes between the microarray and the qPCR ($P = 0.245$) and no significant correlation between the difference and the average of fold changes for these factors ($r = 0.27$, $P = 0.05$), suggesting agreement of the fold changes between them. Consistent with the data from microarray analysis, the qPCR demonstrated significant up-regulation in genes related to cholesterol efflux, significant down-regulation in those involved in development of adrenocortical progenitor cells, and no significant change in those associated with steroid hormone biosynthesis or cholesterol biosynthesis and influx (Table 1).

Iba1 (Afi1) and F4/80 (Emr1) expressions in adrenal glands

We examined an expression pattern of macrophage-specific genes in the adrenal glands by immunohistochemistry at E17.5–18.5 with polyclonal antibodies against Iba1 or monoclonal antibody against F4/80 antigen. Iba1 and F4/80 are both specific markers for macrophages (22,

TABLE 1. Fold change in expression level of genes in knockout mice lacking StAR compared with those in wild-type mice by quantitative real-time PCR

Gene symbol	Description	Fold change (mean ± SE)
Steroid hormone biosynthesis		
Nr5a1	Nuclear receptor subfamily 5, group A, member 1	0.68 ± 0.52
Mc2r	Melanocortin 2 receptor	0.29 ± 0.18
Mrap	Melanocortin 2 receptor accessory protein	0.26 ± 0.51
Star	Steroidogenic acute regulatory protein	0.02 ± 0.01[a]
Cyp11a1	Cytochrome P450, family 11, subfamily a, polypeptide 1	0.63 ± 0.48
Fdx1	Ferredoxin 1	0.63 ± 0.69
Fdxr	Ferredoxin reductase	0.69 ± 0.56
Hsd3b1	Hydroxy-δ-5-steroid dehydrogenase, 3 β- and steroid δ-isomerase 1	0.51 ± 0.53
Agtr1a	Angiotensin II receptor, type 1a	0.76 ± 0.58
Cholesterol biosynthesis and influx		
Ldlr	Low-density lipoprotein receptor	1.58 ± 1.19
Scarb1	Scavenger receptor class B, member 1	1.39 ± 2.91
Hmgcr	3-Hydroxy-3-methylglutaryl-Coenzyme A reductase	0.77 ± 0.31
Lipe	Lipase, hormone sensitive	0.93 ± 0.45
Npc2	Niemann pick type C2	3.46 ± 4.7
Stard3	START domain containing 3	4.69 ± 3.15[a]
Bzrpl1	Benzodiazapine receptor, peripheral-like 1	0.82 ± 0.94
Srebf1	Sterol regulatory element binding factor 1	1.9 ± 0.93
Acat2	Acetyl-coenzyme A acetyltransferase 2	1.19 ± 1.08
Cholesterol metabolism and efflux		
Nr1h2	Nuclear receptor subfamily 1, group H, member 2	3.04 ± 1.21[a]
Nr1h3	Nuclear receptor subfamily 1, group H, member 3	7.76 ± 1.38[a]
Abca1	ATP-binding cassette, subfamily A (ABC1), member 1	2.92 ± 1.59[a]
Abcg1	ATP-binding cassette, subfamily G (WHITE), member 1	5.69 ± 3.1[a]
Abcb1a	ATP-binding cassette, subfamily B (MDR/TAP), member 1A	0.37 ± 0.93
Dhcr24	24-Dehydrocholesterol reductase	0.54 ± 0.62
ch25 h	Cholesterol 25-hydroxylase	0.57 ± 1.69
Adrenocortical development		
Wt1	Wilms tumor homolog	1.83 ± 1.26
Nr0b1	Nuclear receptor subfamily 0, group B, member 1	0.09 ± 0.10[a]
Shh	Sonic hedgehog	0.02 ± 0.02[a]
Wnt4	Wingless-related mouse mammary tumor virus integration site 4	0.08 ± 0.06[a]
Inflammatory response		
Cd86	CD86 antigen	6.44 ± 3.39[a]
Cd36	CD36 antigen	3.29 ± 2.03[a]
Cd5l	CD5 antigen-like	130.95 ± 273.32[a]
Spp1	Secreted phosphoprotein 1	259.15 ± 133.85[a]
Ccl5	Chemokine (C-C motif) ligand 5	113.14 ± 144.27[a]
Cxcl9	Chemokine (C-X-C motif) ligand 9	0.28 ± 1.23
Clec7a	C-type lectin domain family 7, member a	100.69 ± 65.1[a]
H2-Aa	Histocompatibility 2, class II antigen A, α	36.41 ± 147.76
H2-Ab1	Histocompatibility 2, class II antigen A, β1	24.29 ± 70.12
H2-Ea	Histocompatibility 2, class II antigen Eα	37.09 ± 475.29
Tlr1	Toll-like receptor 1	4.12 ± 3.97
Tlr2	Toll-like receptor 2	2.82 ± 2.31
Tlr4	Toll-like receptor 4	2.08 ± 1.24
Tlr6	Toll-like receptor 6	8.2 ± 8.33
Tlr7	Toll-like receptor 7	4.59 ± 3.41

[a] Statistically significant change ($P < 0.05$).

23). As shown in Fig. 2, Iba1 or F4/80 immunoreactivity was identified in only a few SF-1-negative resident macrophages within the adrenal cortex of $Star^{+/+}$ mice. By contrast, in the adrenal cortex of $Star^{-/-}$ mice, immunoreactivity was detected not only in an increased number of SF-1-negative resident macrophages but also for most adrenocortical cells.

Discussion

In this study, we performed transcriptome analysis of eGFP-positive cells selectively purified from adrenal glands in $Star^{-/-}$ mice carrying the StAR/eGFP BAC transgene. StAR regulates the acute phase of steroidogenesis and is expressed throughout the adrenal cortex at E12.5

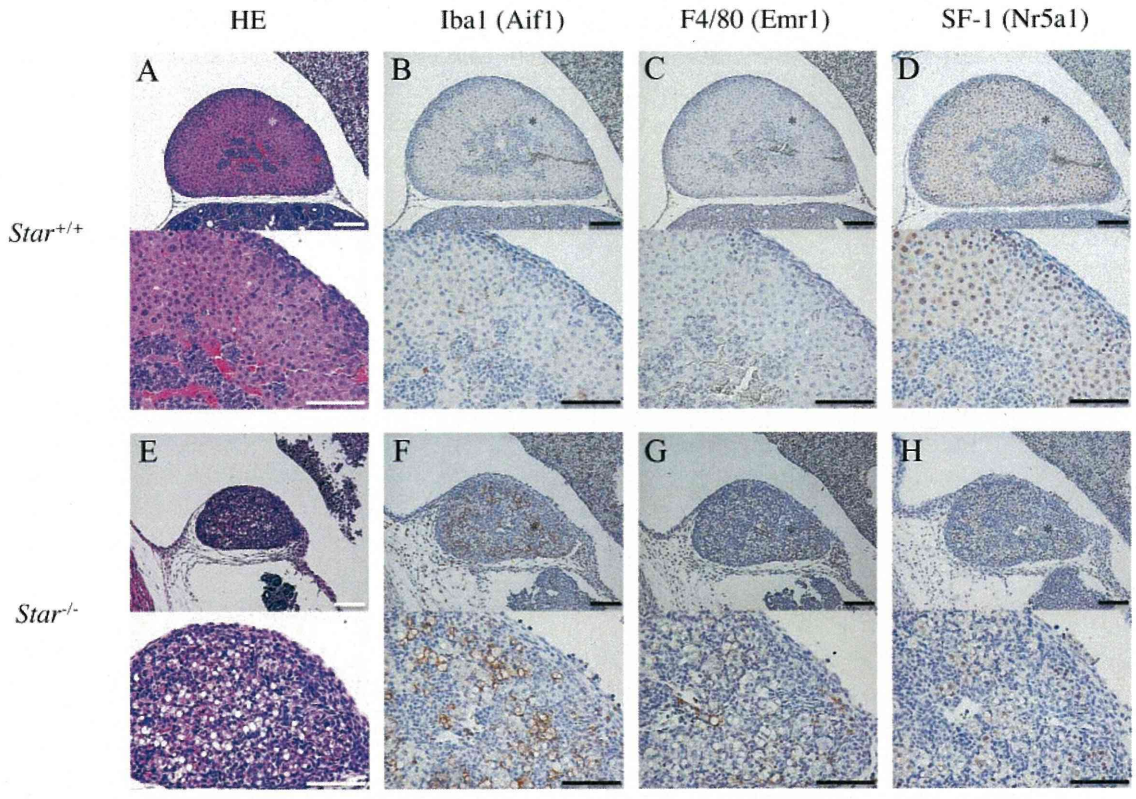

FIG. 2. Expression of macrophage markers in adrenal glands of $Star^{+/+}$ or $Star^{-/-}$ mice at E17.5–18.5 by immunohistochemistry. A–D, $Star^{+/+}$. E–H, $Star^{-/-}$. The *lower panels* show higher magnification of the area around the *asterisk* in the *upper panels*. *Scale bars*, 100 μm.

and later. Indeed, eGFP expression at E17.5 and E18.5 was consistent with endogenous StAR expression in adrenocortical cells as well as fetal Leydig cells. Thus, our experimental data showing 1973 differentially expressed genes convincingly identify the molecular characteristics specific for adrenocortical cells of $Star^{-/-}$ mice.

To clarify the two-hit model for lipoid CAH, we first focused on an expression profile of genes related to cholesterol biosynthesis and influx and steroid hormone biosynthesis. No significant difference was found in the expression of those pathways between the genotypes. ACTH levels of the newborn $Star^{-/-}$ mice were significantly higher than those of the newborn $Star^{+/+}$ mice (Sasaki G., unpublished data). Thus, the up-regulation of signal transduction for melanocortin type 2 receptor (Mc2r) was suppressed in $Star^{-/-}$ mice. This notion is consistent with adrenocortical quiescence that was described as a period of decreased responsiveness to ACTH in the midgestation of fetal sheep (24). In fact, the growth rate of fetal rat adrenal glands actually decreased as term approached (25). By contrast, genes related to cholesterol mobilization and efflux were significantly up-regulated in $Star^{-/-}$ mice. Therefore, although adrenocortical quiescence may be the case, it is inferred that the $Star^{-/-}$ mice-derived adrenocortical cells coordinate the pathways for cholesterol distribution to prevent malfunction due to the accumulation of free cholesterol.

Cummins (26) demonstrated that LXRα and -β (*Nr1h3* and *Nr1h2*, respectively) possessed a pivotal role in preventing the accumulation of free cholesterol in adrenal glands because knockout mice lacking LXRα and -β ($Lxr\alpha\beta^{-/-}$ mice) exhibited cholesterol ester accumulation. Consistent with this notion, the present study revealed the significant up-regulation of LXRα and -β in the adrenocortical cells of $Star^{-/-}$ mice that were full of cholesterol esters in the cytosol. The LXR up-regulation could result from the accumulation of oxysterol intermediates that work as ligands for LXR within the adrenocortical cells of $Star^{-/-}$ mice and lead to an induction of cholesterol efflux by increased expression of ATP-binding cassettes (*Abca1* and *Abcg1*). Furthermore, the increased LXR signaling could inhibit the expression of multiple steroidogenic genes as reported in the H295R human adrenocortical cell line (27). $Lxr\alpha\beta^{-/-}$ mice showed an increased adrenal steroidogenesis, even with a slight increase in StAR expression, indicating the possible link between repression of LXR signaling and increase in StAR-independent steroidogenesis. These findings give additional credence to the

role of LXR in the basal maintenance of adrenal cholesterol homeostasis and also imply the relevance of LXR up-regulation to the loss of residual capacity of StAR-independent steroidogenesis as the second hit of the two-hit model for lipoid CAH.

This study highlights another pathophysiological process likely modulated by StAR deficiency. We found that genes involved in the inflammatory or immune response showed significant positive correlation with the differentially expressed genes in *Star*$^{-/-}$ mice-derived adrenocortical cells. In addition, we identified significantly higher mRNA levels of the epithelial growth factor-like module containing, mucin-like, hormone receptor-like sequence 1 (*Emr1*) and integrin-αX (*Itgax*), markers for total and M1 , respectively. We also confirmed Iba1 or F4/80 (Emr1) immunoreactivity in the adrenal cortex of *Star*$^{-/-}$ mice, suggesting that adrenal steroidogenic cells express certain inflammatory response markers such as macrophages. It may be possible that the cytokine signaling of macrophages modifies the expression or function of molecules involved in steroidogenesis. Woods and Judd (28) previously described that IL-4 signaling inhibited the expression of steroidogenic enzymes induced by ACTH in bovine zona reticularis cells. IL-4 is one of the T-helper 2-type cytokines and is able to activate macrophages in an alternative fashion (29). In fact, IL-4 signaling was one of the canonical pathways in which the genes were significantly up-regulated in *Star*$^{-/-}$ mice. Therefore, the increased inflammatory or immune response, including IL-4 signaling, could be the second hit of the two-hit model for lipoid CAH, attenuating signal transduction of Mc2r under high levels of circulating ACTH.

The present findings also suggest a possible link between the inflammatory or immune system and adrenal glands. The adrenocortical cells produce a variety of cytokines during acute stress (30). The rat adrenal glands have been shown to contain resident macrophages (31, 32). The intraadrenal macrophages were reported to have a major role in affecting adrenal gland function in an autocrine or paracrine fashion (30). As shown in this study, *Star*$^{-/-}$ mice-derived adrenal glands contained a lot of macrophages. It could be possible that *Star*$^{-/-}$ mice-derived adrenocortical cells and resident macrophages interactively affect each other. In fact, *Star*$^{-/-}$ mice-derived adrenocortical cells exhibited significantly higher mRNA levels of chemokine ligand 5 (*Ccl5*) and CD36 antigen (*Cd36*). Chemokine ligand 5, one of the adipocytokines, recruits macrophages into adipose tissues (33). CD36, a receptor of apoptosis inhibitor of macrophage, induces lipolysis and chemokine production in adipocytes (34). These data suggest the adrenal glands in *Star*$^{-/-}$ mice share some of the characteristics of both adipocytes and macrophages in obesity-based chronic, low-grade inflammation of white adipose tissues (35–38), suggesting the possible reciprocal interaction between adrenocortical cells and macrophages in the pathological condition of cholesterol ester accumulation in the cytosol of adrenocortical cells.

The cytokine signals in adrenocortical cells may have a physiological role not only in the stress response but also in the maintenance of homeostasis, monitoring of malfunction, or adaptation to malfunction known as parainflammation (39). In fact, knockout mice lacking toll-like receptor-2 (Tlr2) demonstrated impaired corticosterone secretion at the basal or stress-induced stage and marked cellular disorganization in adrenal gland ultrastructure (40). Tlr2 signaling could be pivotal for sufficient amount of steroidogenesis in adrenal glands. Furthermore, the 3.5-kb StAR mRNA that is predominant in rodent steroidogenic cells contains five classical AU-rich elements in the 3′-untranslated region (41), which has been reported to stabilize mRNA in a number of cytokines involved in chronic inflammation (42). *Star* could share transcriptional regulation through the AU-rich elements with those cytokines. The actual role of parainflammation in adrenocortical cells still remains to be determined. Additional data are required to clarify the functional relevance of those cytokine signals to the physiological condition of adrenocortical cells.

It has recently been reported by the laboratory of Morohashi and colleagues (20, 21) that, by discovering a fetal adrenal-specific enhancer in the *Nr5a1* gene, the mouse adrenal cortex develops two distinct cell types, fetal and adult/definitive zones, during embryonic and early postnatal periods similar to human adrenal glands. The transition from fetal to adult adrenocortical cells was regulated by dosage-sensitive sex reversal-adrenal hypoplasia critical region on the X chromosome 1 (Nr0b1) and other growth factors expressed in the developing definitive zone, including the wingless-related mouse mammary tumor virus integration site 4 (Wnt4) and the sonic hedgehog (Shh) (21, 43–46). At E17.5 and E18.5, the definitive zone develops throughout the adrenal cortex, and the fetal zone remains at the inner part between the definitive zone and medulla. Most cells in the fetal and definitive zones express steroidogenic enzymes and possess the ability to produce steroid hormones at this stage. Thus, our expression profiles at E17.5–18.5 contained characteristics of both fetal and definitive zones. Interestingly, the components related to the transition of fetal to adult adrenocortical cells such as *Nr0b1*, *Wnt4*, and *Shh* were significantly down-regulated in *Star*$^{-/-}$ mice-derived adrenocortical cells. In fact,

the adrenal glands of *Star*$^{-/-}$ mice are hypoplastic in size and disorganized in cortical zonation. These data indicate that decreased expression of these components disturb proliferation and differentiation of the adrenal cortex in *Star*$^{-/-}$ mice.

We recognize the present study possesses potential limitations. First, the expression profile could be modified by excessive physical stress at the moment the animals were killed. We prudently used anesthesia for the pregnant female mice and quickly harvested the adrenal glands from the fetus to minimize physical stress. Second, the expression profile could be affected by the *in vitro* treatment of tissues with chemical digestion. We frequently watched tissues during digestion and ceased the reaction before they were damaged. Third, the expression profile could be biased by sex difference because our data were obtained from both female and male embryos. We did not identify any differentially expressed genes between male and female *Star*$^{+/+}$ embryos (Ishii T., unpublished observation). Finally, we would not rule out the possible recruitment of macrophages into an eGFP-positive cell population because autofluorescence or StAR expression was identified in the macrophages (47, 48). We set the adrenal glands of the *Star*$^{-/-}$ mice carrying no StAR/eGFP transgene as negative controls in FAC sorting. We did not find immunoreactive eGFP among Iba1-positive macrophages in the spleens of mice carrying the StAR/eGFP transgene at E17.5 and E18.5. It is less likely that macrophages in the adrenal cortex were sorted into eGFP-positive cells unless macrophages engulfed eGFP of adrenocortical cells. Given these caveats, the data presented conceivably reflect the pathological features in adrenocortical cells *in vivo* at E17.5–18.5.

In summary, we have demonstrated that StAR deficiency alters the gene expression profile of adrenocortical cells. This includes the significant up-regulation of genes associated with cholesterol efflux, especially LXR, preventing malfunction due to excessive accumulation of intracellular cholesterol, and the significant down-regulation of those regulating the development of adrenocortical zonation, leading to hypoplastic and disorganized structure of adrenal glands. This study also revealed a potentially pivotal role of the inflammatory or immune response in the pathological conditions of adrenocortical cells. This robust approach has expanded our understanding and helped to clarify the pathophysiology of steroidogenic cells with the disruption of StAR.

Acknowledgments

We sincerely dedicate this study to Dr. Keith L. Parker (Division of Endocrinology and Metabolism, Department of Internal Medicine, University of Texas Southwestern Medical Center, Dallas, TX), who passed away on December 12, 2008, after he kindly provided us with knockout mice lacking steroidogenic acute regulatory protein, in token of gratitude and appreciation for his generosity. We would like to thank Drs. Mie Hayashi, Naoko Amano, Masaki Takagi, and Ayuko Suwanai (Department of Pediatrics, School of Medicine, Keio University, Tokyo, Japan) for assistance, Drs. Satoshi Narumi (Department of Pediatrics, School of Medicine, Keio University, Tokyo, Japan), and Goro Sasaki (Department of Pediatrics, Tokyo Dental University, Ichikawa, Japan) for helpful discussion, Ms. Mari Fujiwara (the Core Instrumentation Facility, School of Medicine, Keio University, Tokyo, Japan) for microarray analysis, and Dr. Gareth Lavery (Centre for Endocrinology, Diabetes and Metabolism, Institute of Biomedical Research, University of Birmingham, Birmingham, UK) for reviewing the manuscript.

Address all correspondence and requests for reprints to: Tomohiro Ishii, M.D., Ph.D., Department of Pediatrics, School of Medicine, Keio University, 35 Shinanomachi, Shinjuku-ku, Tokyo 160-8582, Japan. E-mail: tishii@1992.jukuin.keio.ac.jp.

This work was supported by a Grant-in-Aid for Scientific Research (C) from the Japan Society for the Promotion of Science and a Research Grant from the Yamaguchi Endocrine Research Foundation.

Disclosure Summary: The authors have nothing to disclose.

References

1. **Cherradi N, Rossier MF, Vallotton MB, Timberg R, Friedberg I, Orly J, Wang XJ, Stocco DM, Capponi AM** 1997 Submitochondrial distribution of three key steroidogenic proteins (steroidogenic acute regulatory protein and cytochrome p450scc and 3β-hydroxysteroid dehydrogenase isomerase enzymes) upon stimulation by intracellular calcium in adrenal glomerulosa cells. J Biol Chem 272:7899–7907
2. **Stocco DM, Clark BJ, Reinhart AJ, Williams SC, Dyson M, Dassi B, Walsh LP, Manna PR, Wang XJ, Zeleznik AJ, Orly J** 2001 Elements involved in the regulation of the StAR gene. Mol Cell Endocrinol 177:55–59
3. **Stocco DM** 2001 StAR protein and the regulation of steroid hormone biosynthesis. Annu Rev Physiol 63:193–213
4. **Artemenko IP, Zhao D, Hales DB, Hales KH, Jefcoate CR** 2001 Mitochondrial processing of newly synthesized steroidogenic acute regulatory protein (StAR), but not total StAR, mediates cholesterol transfer to cytochrome P450 side chain cleavage enzyme in adrenal cells. J Biol Chem 276:46583–46596
5. **Jefcoate C** 2002 High-flux mitochondrial cholesterol trafficking, a specialized function of the adrenal cortex. J Clin Invest 110:881–890
6. **Bose HS, Lingappa VR, Miller WL** 2002 Rapid regulation of steroidogenesis by mitochondrial protein import. Nature 417:87–91
7. **Miller WL, Auchus RJ** 2011 The molecular biology, biochemistry, and physiology of human steroidogenesis and its disorders. Endocr Rev 32:81–151
8. **Bose HS, Sugawara T, Strauss 3rd JF, Miller WL** 1996 The pathophysiology and genetics of congenital lipoid adrenal hyperplasia. International Congenital Lipoid Adrenal Hyperplasia Consortium. N Engl J Med 335:1870–1878

9. **Hasegawa T, Zhao L, Caron KM, Majdic G, Suzuki T, Shizawa S, Sasano H, Parker KL** 2000 Developmental roles of the steroidogenic acute regulatory protein (StAR) as revealed by StAR knockout mice. Mol Endocrinol 14:1462–1471
10. **Ishii T, Hasegawa T, Pai CI, Yvgi-Ohana N, Timberg R, Zhao L, Majdic G, Chung BC, Orly J, Parker KL** 2002 The roles of circulating high-density lipoproteins and trophic hormones in the phenotype of knockout mice lacking the steroidogenic acute regulatory protein. Mol Endocrinol 16:2297–2309
11. **Sasaki G, Ishii T, Jeyasuria P, Jo Y, Bahat A, Orly J, Hasegawa T, Parker KL** 2008 Complex role of the mitochondrial targeting signal in the function of steroidogenic acute regulatory protein revealed by bacterial artificial chromosome transgenesis *in vivo*. Mol Endocrinol 22:951–964
12. **Arakane F, Kallen CB, Watari H, Foster JA, Sepuri NB, Pain D, Stayrook SE, Lewis M, Gerton GL, Strauss 3rd JF** 1998 The mechanism of action of steroidogenic acute regulatory protein (StAR). StAR acts on the outside of mitochondria to stimulate steroidogenesis. J Biol Chem 273:16339–16345
13. **Reiner A, Yekutieli D, Benjamini Y** 2003 Identifying differentially expressed genes using false discovery rate controlling procedures. Bioinformatics 19:368–375
14. **Shi L, Campbell G, Jones WD, Campagne F, Wen Z, Walker SJ, Su Z, Chu TM, Goodsaid FM, Pusztai L, Shaughnessy Jr JD, Oberthuer A, Thomas RS, Paules RS, Fielden M, Barlogie B, Chen W, Du P, Fischer M, Furlanello C, Gallas BD, Ge X, Megherbi DB, Symmans WF, Wang MD, *et al.*** 2010 The MicroArray Quality Control (MAQC)-II study of common practices for the development and validation of microarray-based predictive models. Nat Biotechnol 28:827–838
15. **Shi L, Reid LH, Jones WD, Shippy R, Warrington JA, Baker SC, Collins PJ, de Longueville F, Kawasaki ES, Lee KY, Luo Y, Sun YA, Willey JC, Setterquist RA, Fischer GM, Tong W, Dragan YP, Dix DJ, Frueh FW, Goodsaid FM, Herman D, Jensen RV, Johnson CD, Lobenhofer EK, Puri RK, *et al.*** 2006 The MicroArray Quality Control (MAQC) project shows inter- and intraplatform reproducibility of gene expression measurements. Nat Biotechnol 24:1151–1161
16. **Kupershmidt I, Su QJ, Grewal A, Sundaresh S, Halperin I, Flynn J, Shekar M, Wang H, Park J, Cui W, Wall GD, Wisotzkey R, Alag S, Akhtari S, Ronaghi M** 2010 Ontology-based meta-analysis of global collections of high-throughput public data. PLoS ONE 5:e13066
17. **Bouma GJ, Hart GT, Washburn LL, Recknagel AK, Eicher EM** 2004 Using real time RT-PCR analysis to determine multiple gene expression patterns during XX and XY mouse fetal gonad development. Gene Expr Patterns 5:141–149
18. **Vandesompele J, De Preter K, Pattyn F, Poppe B, Van Roy N, De Paepe A, Speleman F** 2002 Accurate normalization of real-time quantitative RT-PCR data by geometric averaging of multiple internal control genes. Genome Biol 3:RESEARCH0034-RESEARCH0034.0011
19. **Bland JM, Altman DG** 2003 Applying the right statistics: analyses of measurement studies. Ultrasound Obstet Gynecol 22:85–93
20. **Zubair M, Ishihara S, Oka S, Okumura K, Morohashi K-I** 2006 Two-step regulation of Ad4BP/SF-1 gene transcription during fetal adrenal development: initiation by a Hox-Pbx1-Prep1 complex and maintenance via autoregulation by Ad4BP/SF-1. Mol Cell Biol 26: 4111–4121
21. **Zubair M, Parker KL, Morohashi K-I** 2008 Developmental links between the fetal and adult zones of the adrenal cortex revealed by lineage tracing. Mol Cell Biol 28:7030–7040
22. **Kanazawa H, Ohsawa K, Sasaki Y, Kohsaka S, Imai Y** 2002 Macrophage/microglia-specific protein Iba1 enhances membrane ruffling and Rac activation via phospholipase C-γ-dependent pathway. J Biol Chem 277:20026–20032
23. **Lin HH, Stacey M, Stein-Streilein J, Gordon S** 2011 F4/80: the macrophage-specific adhesion-GPCR and its role in immunoregulation. Adv Exp Med Biol 706:149–156
24. **Boshier DP, Holloway H** 1989 Morphometric analyses of adrenal gland growth in fetal and neonatal sheep. I. The adrenal cortex. J Anat 167:1–14
25. **Bertholet JY** 1980 Proliferative activity and cell migration in the adrenal cortex of fetal and neonatal rats: an autoradiographic study. J Endocrinol 87:1–9
26. **Cummins CL, Volle DH, Zhang Y, McDonald JG, Sion B, Lefrançois-Martinez AM, Caira F, Veyssière G, Mangelsdorf DJ, Lobaccaro JM** 2006 Liver X receptors regulate adrenal cholesterol balance. J Clin Invest 116:1902–1912
27. **Nilsson M, Stulnig TM, Lin CY, Yeo AL, Nowotny P, Liu ET, Steffensen KR** 2007 Liver X receptors regulate adrenal steroidogenesis and hypothalamic-pituitary-adrenal feedback. Mol Endocrinol 21:126–137
28. **Woods AM, Judd AM** 2008 Interleukin-4 increases cortisol release and decreases adrenal androgen release from bovine adrenal cells. Domest Anim Endocrinol 34:372–382
29. **Gordon S, Martinez FO** 2010 Alternative activation of macrophages: mechanism and functions. Immunity 32:593–604
30. **Bornstein SR, Rutkowski H, Vrezas I** 2004 Cytokines and steroidogenesis. Mol Cell Endocrinol 215:135–141
31. **Sato T** 1998 Class II MHC-expressing cells in the rat adrenal gland defined by monoclonal antibodies. Histochem Cell Biol 109:359–367
32. **Schober A, Huber K, Fey J, Unsicker K** 1998 Distinct populations of macrophages in the adult rat adrenal gland: a subpopulation with neurotrophin-4-like immunoreactivity. Cell Tissue Res 291:365–373
33. **Keophiphath M, Rouault C, Divoux A, Clément K, Lacasa D** 2010 CCL5 promotes macrophage recruitment and survival in human adipose tissue. Arterioscler Thromb Vasc Biol 30:39–45
34. **Kurokawa J, Nagano H, Ohara O, Kubota N, Kadowaki T, Arai S, Miyazaki T** 2011 Apoptosis inhibitor of macrophage (AIM) is required for obesity-associated recruitment of inflammatory macrophages into adipose tissue. Proc Natl Acad Sci USA 108:12072–12077
35. **Gregor MF, Hotamisligil GS** 2011 Inflammatory mechanisms in obesity. Annu Rev Immunol 29:415–445
36. **Suganami T, Ogawa Y** 2010 Adipose tissue macrophages: their role in adipose tissue remodeling. J Leukoc Biol 88:33–39
37. **Trayhurn P, Wood IS** 2004 Adipokines: inflammation and the pleiotropic role of white adipose tissue. Br J Nutr 92:347–355
38. **Cottam DR, Mattar SG, Barinas-Mitchell E, Eid G, Kuller L, Kelley DE, Schauer PR** 2004 The chronic inflammatory hypothesis for the morbidity associated with morbid obesity: implications and effects of weight loss. Obes Surg 14:589–600
39. **Medzhitov R** 2008 Origin and physiological roles of inflammation. Nature 454:428–435
40. **Bornstein SR, Zacharowski P, Schumann RR, Barthel A, Tran N, Papewalis C, Rettori V, McCann SM, Schulze-Osthoff K, Scherbaum WA, Tarnow J, Zacharowski K** 2004 Impaired adrenal stress response in Toll-like receptor 2-deficient mice. Proc Natl Acad Sci USA 101:16695–16700
41. **Zhao D, Duan H, Kim YC, Jefcoate CR** 2005 Rodent StAR mRNA is substantially regulated by control of mRNA stability through sites in the 3′-untranslated region and through coupling to ongoing transcription. J Steroid Biochem Mol Biol 96:155–173
42. **Khabar KSA** 2010 Post-transcriptional control during chronic inflammation and cancer: a focus on AU-rich elements. Cell Mol Life Sci 67:2937–2955

43. **Kim AC, Barlaskar FM, Heaton JH, Else T, Kelly VR, Krill KT, Scheys JO, Simon DP, Trovato A, Yang WH, Hammer GD** 2009 In search of adrenocortical stem and progenitor cells. Endocr Rev 30: 241–263
44. **King P, Paul A, Laufer E** 2009 Shh signaling regulates adrenocortical development and identifies progenitors of steroidogenic lineages. Proc Natl Acad Sci USA 106:21185–21190
45. **Huang CC, Miyagawa S, Matsumaru D, Parker KL, Yao HH** 2010 Progenitor cell expansion and organ size of mouse adrenal is regulated by sonic hedgehog. Endocrinology 151:1119–1128
46. **Ching S, Vilain E** 2009 Targeted disruption of Sonic Hedgehog in the mouse adrenal leads to adrenocortical hypoplasia. Genesis 47:628–637
47. **Ma Y, Ren S, Pandak WM, Li X, Ning Y, Lu C, Zhao F, Yin L** 2007 The effects of inflammatory cytokines on steroidogenic acute regulatory protein expression in macrophages. Inflamm Res 56:495–501
48. **ten Hagen TL, van Vianen W, Bakker-Woudenberg IA** 1996 Isolation and characterization of murine Kupffer cells and splenic macrophages. J Immunol Methods 193:81–91